Earth-Science Reviews 134 (2014) 81–97

Contents lists available at ScienceDirect

Earth-Science Reviews

journal homepage: www.elsevier.com/locate/earscirev

Organic-rich sedimentation in the South Pacific Ocean associated with Late Paleocene climatic cooling

Christopher J. Hollis [a,*], Michael J.S. Tayler [b], Benjamin Andrew [b], Kyle W. Taylor [c], Pontus Lurcock [d], Peter K. Bijl [f], Denise K. Kulhanek [a,g], Erica M. Crouch [a], Campbell S. Nelson [b], Richard D. Pancost [c], Matthew Huber [h], Gary S. Wilson [d], G. Todd Ventura [a], James S. Crampton [a], Poul Schiøler [a,i], Andy Phillips [a,e]

[a] GNS Science, PO Box 30-368, Lower Hutt, New Zealand
[b] Department of Earth Sciences, University of Waikato, Hamilton, New Zealand
[c] Bristol Biogeochemistry Research Centre, University of Bristol, Bristol BS8 1TS, United Kingdom
[d] Geology Department, University of Otago, Dunedin, New Zealand
[e] Victoria University of Wellington, Wellington, New Zealand
[f] Laboratory of Palaeobotany and Palynology, Department of Earth Science, Utrecht University, 3584 CD Utrecht, The Netherlands
[g] Integrated Ocean Drilling Program, Texas A&M University, TX 77845-9547, United States
[h] Department of Earth Sciences, University of New Hampshire, Durham, NH 03824-3525, United States
[i] Morgan Goodall Palaeo, Box 161, Maitland, SA 5373, Australia

A R T I C L E I N F O

Article history:
Received 23 June 2013
Accepted 14 March 2014
Available online 22 March 2014

Keywords:
Paleogene
Paleoclimate
Regional cooling
Sea level fall
Organic facies
Geochemistry

A B S T R A C T

A distinctive organic-rich marine mudstone of Late Paleocene age occurs in most of New Zealand's sedimentary basins and has been identified as a potential source rock for oil and gas. Identified as the Waipawa Formation in the East Coast Basin and the Tartan Formation in the Great South and Canterbury Basins, the unit is a relatively uniform massive mudstone that varies greatly in thickness (2–70 m) and grades laterally into distinctive facies equivalents, notably greensand and a thin-bedded siliceous mudstone. All these facies are characterised by relatively high TOC (0.5–10 wt.%) and ^{13}C enrichment ($\delta^{13}C_{TOC} > -24‰$), and we refer to them collectively as "Waipawa organofacies". Our detailed stratigraphic and geochemical studies refine the age (58.7 to 59.4 Ma), distribution and nature of the Waipawa organofacies. We have determined that deposition occurred in continental margin settings throughout much of the southwest Pacific under cool, dysoxic conditions associated with a significant influx of terrestrial organic matter, high marine productivity, a global fall in sea level, and a regional unconformity across shallow and deep marine settings. The combination of cool temperatures, lowered sea level and bathyal erosion suggests that deposition was linked to short-lived growth of an Antarctic ice sheet in the earliest Late Paleocene (~59 Ma).

Contents

* Corresponding author. Tel.: +64 4 570 4868; fax: +64 4 570 4600.
E-mail address: c.hollis@gns.cri.nz (C.J. Hollis).

http://dx.doi.org/10.1016/j.earscirev.2014.03.006
0012-8252/

1. Introduction

Organic-rich marine sediments are of interest for both economic and environmental reasons. As well as being important sources of oil and gas, their deposition signals distinct environmental conditions that have been associated with global climatic events (e.g. Schlanger and Jenkyns, 1976). However, in many cases the nature and causes of these events remain enigmatic (e.g. Barclay et al., 2010; Spofforth et al., 2010; Jarvis et al., 2011). The widespread occurrence of a Late Paleocene organic-rich mudstone in the New Zealand region (Fig. 1) has been the focus of considerable research, both in relation to its petroleum source rock potential (Moore, 1988, 1989; Field et al., 1997; Killops et al., 1997; Hollis and Manzano-Kareah, 2005; Schiøler et al., 2010) and its significance for climatic changes in the greenhouse world of the early Cenozoic (Leckie et al., 1995; Killops et al., 2000; Hollis et al., 2005a). However, there has been little agreement on the depositional setting of the unit, with some arguing for a setting within a deep-water oxygen minimum zone (Leckie et al., 1995; Killops et al., 2000; Rogers et al., 2001; Hollis et al., 2005a) and others suggesting a more restricted, shallow marine setting (Moore, 1988; Schiøler et al., 2010).

This organic-rich rock unit is identified as the Waipawa Formation in eastern North Island sedimentary basins, where it has been recorded from southeast Wairarapa (Moore, 1988; Lee and Begg, 2002) to Northland (Isaac et al., 1994; Hollis et al., 2006) (Figs. 1, 2). In the sedimentary basins of southeast South Island, a correlative unit is identified as the Tartan Formation (Cook et al., 1999; Schiøler et al., 2010). Coeval units in northeast South Island and further afield have been informally correlated with the Waipawa Formation (Killops et al., 2000; Hollis et al., 2005a). Here we review published records of these units, which we refer to collectively as "Waipawa organofacies"; we present new stratigraphic and geochemical data for key sections, and we discuss the implications for its age, depositional setting and origin. We show that deposition of Waipawa organofacies is linked to sea level fall and climatic cooling and we argue that this implies that ice sheets grew on Antarctica in the earliest Late Paleocene (~59 Ma).

2. Material and methods

2.1. Localities and samples

Four types of stratigraphic record form the basis of this study (Fig. 2): (i) stratigraphic sections of typical Waipawa Formation from the East Coast Basin [Te Hoe River and Angora Road (Moore, 1988)]; (ii) sections with correlative, moderately organic-rich, yet distinct lithotypes from the East Coast and Canterbury Basins [Tawanui (Moore, 1988; Rogers et al., 2001), Toi Flat (Crouch et al., 2014), Mead Stream (Hollis et al., 2005a) and mid-Waipara River (Morgans et al., 2005; Hollis et al., 2009, 2012)]; (iii) offshore records of time-equivalent intervals in marine sediment cores [Deep Sea Drilling Project (DSDP) Site 277, western Campbell Plateau (Kennett et al., 1975; Hollis et al., 1997a), Ocean Drilling Program (ODP) Site 1121, eastern Campbell Plateau (Carter et al., 1999; Hollis, 2002; Wei et al, 2005) and ODP Site 1172, East Tasman Plateau (Exon et al., 2001; Röhl et al., 2004; Bijl et al., 2009)]; and (iv) sections that include correlated unconformities, primarily in the southern East Coast Basin [Kaikoura, Muzzle and Bluff Streams (Hollis et al., 2005b), but also on the subantarctic Campbell Plateau (Beggs, 1978; Hollis et al., 1997a,b)]. New data are presented for the following sections, which were logged by tape and compass: Angora Road, Tawanui, Mead Stream, Kaikoura (Wharf section), mid-Waipara River (Column 2), and Limestone Point (Campbell Island). Petrological, sedimentological, paleontological and geochemical studies have been carried out on Angora, Tawanui, Mead, Muzzle, Kaikoura and Campbell Island sections (Andrew, 2010; Tayler, 2011; Taylor, 2011). Biostratigraphic and geochemical studies undertaken here for the Paleocene intervals at DSDP Site 277 and ODP Sites 1121 and 1172 complement earlier studies (Hollis et al., 1997b; Hollis, 2002; Röhl et al., 2004; Wei et al., 2005; Bijl et al., 2009, 2010; Taylor, 2011). The Campbell Island and mid-Waipara sections were also sampled for paleomagnetic study (Lurcock, 2012). Stratigraphic descriptions of individual sections are provided in the Supplementary materials.

2.2. Age and correlation

Waipawa Formation is typically non-calcareous and its bounding units are commonly also non-calcareous or weakly calcareous, which makes dating by foraminifera or calcareous nannofossils difficult. In this study, we utilise a new Paleocene dinoflagellate cyst (dinocysts) biozonation (Crouch et al., 2014), which is calibrated to the 2012 International Timescale (Gradstein et al., 2012) by means of calcareous nannofossil datums within calcareous intervals in the Tawanui, Angora and mid-Waipara sections and ODP Site 1121, eastern Campbell Plateau. Radiolarians and planktic foraminifera provide additional age control at ODP Site 1121 and Mead Stream (Hollis, 2002; Hollis et al., 2005a,b). Magnetostratigraphy is used to refine age control at ODP Site 1172 (Röhl et al., 2004; Bijl et al., 2009, 2010), and at mid-Waipara River and Campbell Island (Lurcock, 2012). Nannofossils are used to date the Paleocene unconformity at DSDP Site 277. Biostratigraphic and magnetostratigraphic events are used to develop age models and sedimentation rate curves for Angora, mid-Waipara River, and ODP Sites 1121 and 1172.

2.3. Inorganic geochemistry

Elemental data for the mid-Waipara and Angora sections were obtained using a Spectro X-Lab fully automated X-Ray Fluorescence (XRF) spectrometer at the University of Waikato. Error for major elements is $\pm$5% and for minor elements error varies from 1 to 5% depending on the element and its abundance; errors are <1% for Ba and S and ~5% for Mo.

2.4. Stable isotopes and TOC

Total organic carbon (TOC) and bulk organic $\delta^{13}C$ ($\delta^{13}C_{TOC}$) analyses were undertaken at two laboratories. Mid-Waipara samples were analysed at Isotrace, Dunedin, New Zealand. Samples from ODP Sites 1121 and 1172 were analysed at the GNS Science Stable Isotope Laboratory, Lower Hutt, New Zealand. All $\delta^{13}C$ results are reported in per mil (‰) notation relative to the Vienna Peedee Belemnite (VPDB) standard. Analytical precision was measured at $\pm$0.15‰ for $\delta^{13}C_{TOC}$.

2.5. Glycerol dialkyl glycerol tetraethers (GDGTs)

Analysis of samples was undertaken at two laboratories. Samples from Mid-Waipara and ODP Site 1121 were analysed in the Organic Geochemistry Unit at Bristol University and results for mid-Waipara have been reported by Hollis et al. (2012) and Pancost et al. (2013). Samples from ODP Site 1172 were analysed in the Laboratory of Palynology and Palaeobotany at Utrecht University and include a low resolution sample suite reported by Bijl et al. (2009) and a higher resolution suite presented in this study. Sea surface temperatures (SSTs) were calculated from GDGTs using the calibrations of Kim et al. (2010): TEX^H_{86} and TEX^L_{86}. TEX^H_{86} comprises the same combination of GDGTs as in the original TEX_{86} proxy (Schouten et al., 2002) but is based on a log relationship rather than linear (e.g., Schouten et al., 2002; Kim et al., 2008) or reciprocal (Liu et al., 2009) relationships. The calibration with SST is based on a low- to mid-latitude core-top data set and the TEX^H_{86} proxy is recommended for SST records above 15 °C (Kim et al., 2010). TEX^L_{86} comprises a different combination of GDGTs and its calibration to SST is based on a global core-top sediment dataset that includes high-latitude locations. Kim et al. (2010) recommend the use of this proxy for paleo-SST records that include temperatures below 15 °C. The analytical precision of TEX_{86}-based SST reconstructions, based on 1 standard deviation of replicate analyses, is typically c. ±0.3 °C. Calibration errors for TEX^H_{86} and TEX^L_{86} are ±2.5 °C and ±4 °C, respectively. Hollis et al. (2012) developed a preliminary paleo-calibration for TEX_{86} ($pTEX_{86}$) based on

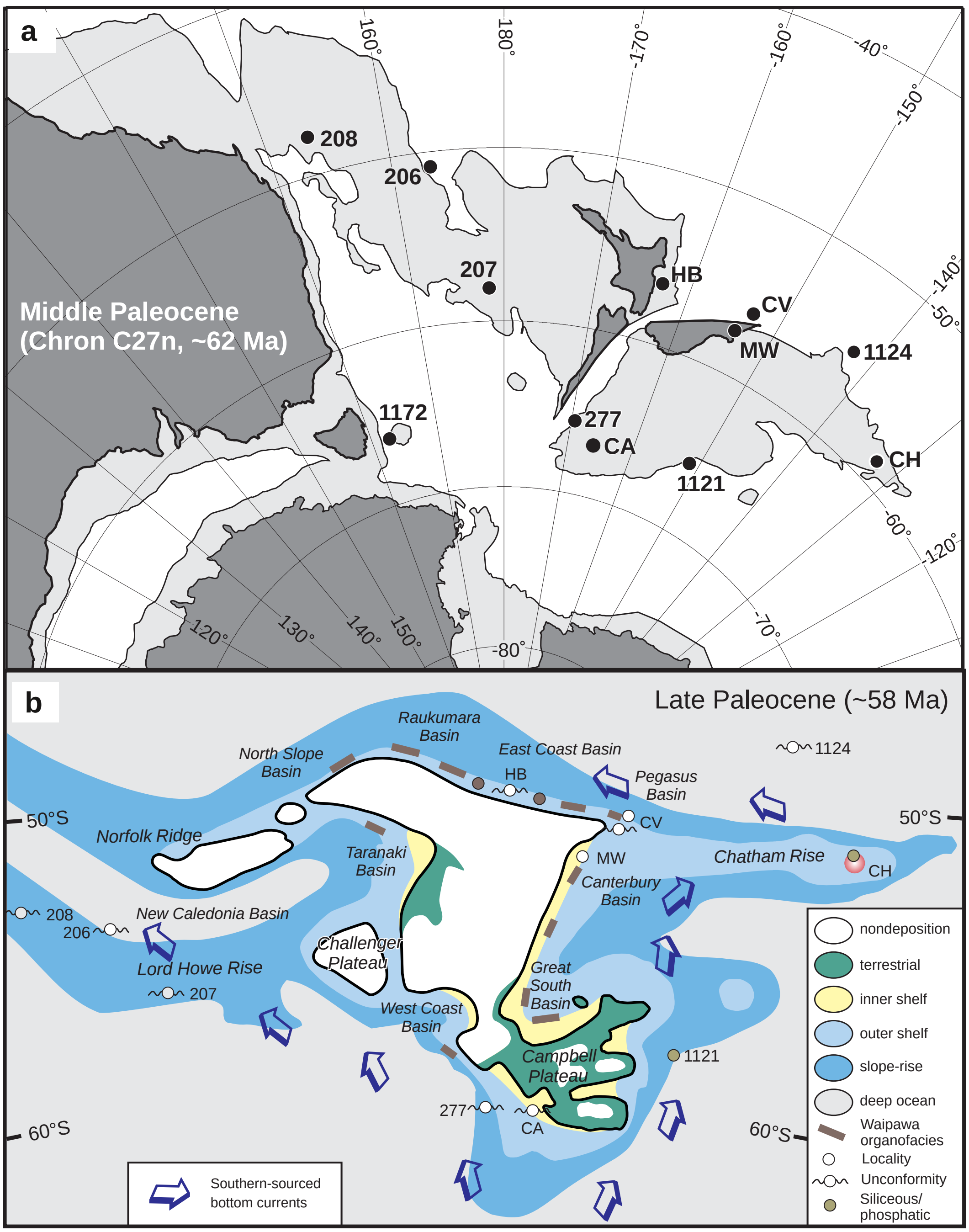

Fig. 1. (a) Tectonic reconstruction for the southwest Pacific in the Middle Paleocene (~62 Ma), adapted from Cande and Stock (2004), and (b) a paleogeographic reconstruction for the New Zealand region in the Late Paleocene (~58 Ma), adapted from King et al. (1999), showing the distribution of Waipawa organofacies. HB, Hawke's Bay; CV, Clarence valley; MW, Mid-Waipara River; CH, Chatham Islands; CA, Campbell Island; numbers are DSDP/ODP sites.

Eocene SST estimates derived from inorganic proxies and demonstrated that, for Southwest Pacific Paleogene records, SST derived from TEX^{L}_{86} exhibits the best fit with SSTs derived from planktic foraminiferal $\delta^{18}O$ values and Mg/Ca ratios. Several issues have been raised with respect to biological, seasonal or water column biases in the SSTs recorded by sedimentary GDGT distributions (e.g., Turich et al., 2007; Kim et al., 2008; Schouten et al., 2013; Taylor et al., 2013). TEX_{86} values can also be compromised by the input of terrestrial GDGTs (Weijers et al., 2007). This influence is thought to be minimal when the branched isoprenoid tetraether vs chenarchaeol (BIT) index, which is an indicator of the relative contribution of terrestrial GDGTs, is lower than 0.3 (Hopmans et al., 2004). The distribution of branched GDGTs has been used to estimate mean annual air temperature (MAAT) in the mid-Waipara section (Pancost et al., 2013). We use the calibration for the MBT′–CBT proxy for MAAT described by Peterse et al. (2012).

3. Results and discussion

3.1. Waipawa organofacies

Waipawa Formation sensu stricto is a poorly-bedded to massive, bioturbated, dark brown-grey mudstone or muddy sandstone, which is commonly glauconitic and often develops a yellow jarositic coating on weathered, sheltered outcrops (Moore, 1988, 1989). Because the type section at Waipawa is poorly exposed, Moore (1988, 1989) designated several reference sections in Hawke's Bay, including Te Hoe River (now also poorly exposed) and Angora Road. The formation has distinctive geochemical characteristics: high TOC (1–12 wt.%, mean of 3.6 wt.%), isotopically heavy $\delta^{13}C_{TOC}$ (>−24‰) and abundant 24-n-propylcholestanes (20–55% of C_{27}–C_{30} regular steranes) (Killops et al., 2000; Hollis and Manzano-Kareah, 2005). Although the unit typically lacks age-diagnostic fossils, an early Late Paleocene age has been inferred from age control in formations above and below (Moore, 1988; Hollis et al., 2005a). The coeval Tartan Formation in the Great South Basin has very similar lithological and geochemical characteristics (Cook et al., 1999; Schiøler et al., 2010) and has been traced into the adjacent Canterbury Basin (Schiøler et al., 2010). Equivalent units have also been identified in the West Coast, Taranaki and North Slope Basins (Killops et al., 2000; Hollis et al., 2006).

In addition to these occurrences of typical Waipawa Formation, we correlate two distinct lithotypes with the formation. In the upper reaches of the Akitio River at Tawanui, Southern Hawke's Bay, the uppermost ~2 m-thick sandstone unit in the Paleocene Te Uri Member (uppermost member of the Whangai Formation in this section) is correlated with Waipawa Formation based on its geochemistry (Fig. 3c). This unit differs from typical Waipawa Formation by being highly glauconitic and only slightly enriched in TOC. In line with the original study by Rogers et al. (2001), we find that the basal part of the unit has low TOC and normal $d^{13}C$ values of −25‰; TOC increases and $\delta^{13}C_{TOC}$ becomes more positive towards the top of the unit. A similar interval of high TOC is identified from a single sample near the top of the Te Uri Member within a drill core from Toi Flat, 7 km ENE of Tawanui (Crouch et al., 2014). At Mead Stream, Marlborough (Fig. 3d), an interval comprising two mudstone units with an intervening siliceous limestone unit has been identified as Waipawa Formation based on the geochemical characteristics of the two mudstones (Killops et al., 2000;

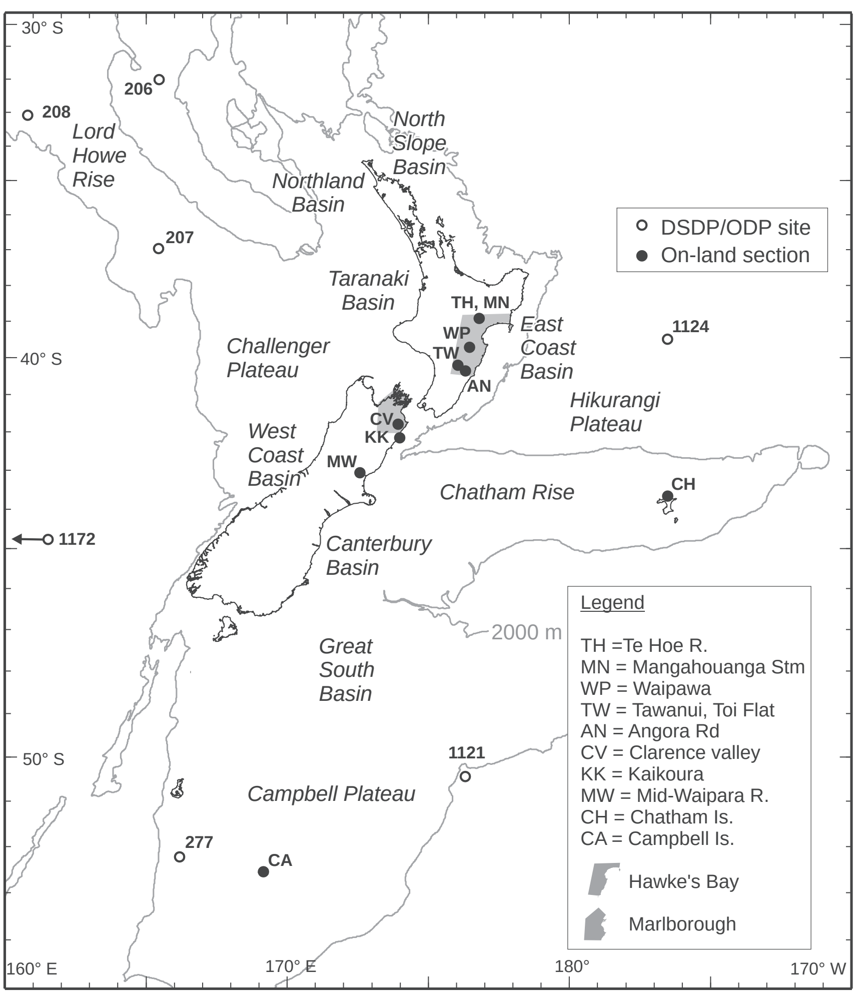

Fig. 2. Locality map of the New Zealand region showing the onshore sections and offshore drill holes referred to in this study.

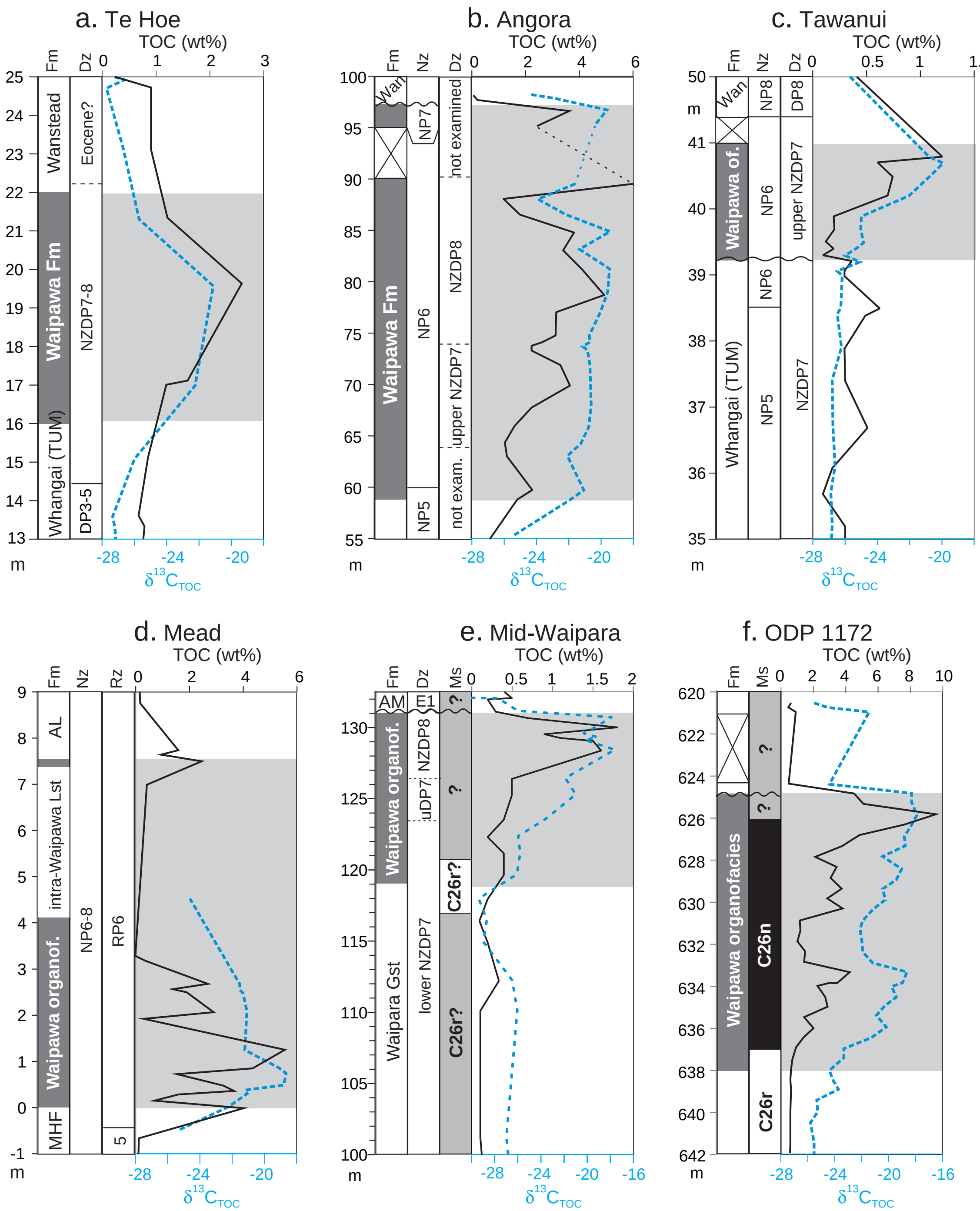

Fig. 3. Relationship between total organic carbon (TOC, black line) and $\delta^{13}C_{TOC}$ (blue dashed line) within the Waipawa Formation in the (a) Te Hoe River and (b) Angora Road sections (northern and southern Hawke's Bay) and within Waipawa organofacies in the (c) Tawanui (southern Hawke's Bay), (d) Mead Stream (Clarence valley, eastern Marlborough), and (e) mid-Waipara (northern Canterbury) sections, and (f) ODP Site 1172 (East Tasman Plateau). Nz, Nannofossil Zone; Dz, Dinocyst Zone; Ms, Magnetostratigraphy. (For interpretation of the references to color in this figure legend, the reader is referred to the web version of this article.)

Hollis et al., 2005a). However, this interval differs from typical Waipawa Formation in several respects. It is well-bedded, includes a 3 m-thick limestone unit, and contains abundant radiolarians and rare foraminifera (Hollis et al., 2005a). Herein, we refer to the typical Waipawa lithotype and these two correlative lithotypes as "Waipawa organofacies". We define Waipawa organofacies as a non-calcareous to weakly calcareous mudstone or muddy sandstone of Late Paleocene age with moderately high to high TOC (0.5–12 wt.%) and relatively enriched in ^{13}C ($\delta^{13}C_{TOC} > -24‰$).

We have confirmed and refined the primary geochemical character of Waipawa organofacies at four of these localities (Te Hoe River, Angora Road, Tawanui and Mead Stream) and identified the organofacies at two new localities (Fig. 3): the mid-Waipara River section, northern Canterbury Basin (Hollis et al., 2009, 2012), and at ODP Site 1172, East Tasman Plateau (Röhl et al., 2004; Bijl et al., 2009). At these six localities, a ~2 to ~40 m-thick interval of dark grey to brown-grey mudstone or fine sandstone is identified as Waipawa organofacies based on its geochemical character and age (Fig. 3). The interval correlated with Waipawa organofacies at Site 1172 shows a high γ-ray response and is also enriched in uranium and thorium (Exon et al., 2001), which is consistent with high organic content (Röhl et al., 2004). It is significant that several records of Waipawa organofacies include a zone of lower TOC, more negative $\delta^{13}C$ and usually higher carbonate content. This is most clearly developed at Mead Stream where there are two distinct mudstone units separated by siliceous limestone, but Angora Road and ODP Site 1172 also exhibit this feature (Fig. 3).

Waipawa organofacies appears to have been deposited at a wide range of water depths: from inner to middle shelf in Great South and Canterbury basins (Schiøler et al., 2010) to outer shelf-upper slope in much of the East Coast Basin (Killops et al., 2000). Moore (1988) suggested that the Waipawa Formation was deposited on the inner shelf in the East Coast Basin, based largely on its depauperate agglutinated foraminiferal assemblage. However, the taxa present are indicative of bathyal or greater depths (Killops et al., 2000).

3.2. Organic matter: source, preservation and significance

The correlation between TOC and $\delta^{13}C_{TOC}$ in the Waipawa organofacies has lacked a definitive explanation. Killops et al. (2000) suggested that the correlation may be related to enhanced marine productivity, which would lead to both an increase in deposition of organic matter (OM) and a positive excursion in $\delta^{13}C_{TOC}$ due to surface water depletion of CO_2 (Hollander et al., 1993). Röhl et al. (2004) suggested that the positive $\delta^{13}C_{TOC}$ excursion at ODP Site 1172 may be related to a change in the source of OM. Present-day marine OM typically has a more positive $\delta^{13}C$ value than terrestrial OM (Hayes, 1993; Rullkötter, 2000). However, the high pCO_2 levels of early Paleogene ocean waters appear to have resulted in marine OM with much more depleted $\delta^{13}C$ (c. −26 to −28‰) relative to terrestrial OM values of c. −24‰ (Sluijs and Dickens, 2012). Thus, either enhanced productivity or increased input of terrestrial OM may explain the positive excursion in $\delta^{13}C_{TOC}$ observed in the Waipawa Formation. Although there is biomarker evidence for increased contributions of marine OM in some settings (Killops et al., 2000) and palynofacies evidence for increased terrestrial OM in other settings (Schiøler et al., 2010), neither process appears to be able to account for the a positive excursion in $\delta^{13}C_{TOC}$ in the range of 5 to 10‰. Sinninghe Damsté et al. (1998) observed a similar phenomenon in the Jurassic Kimmeridge Clay and argued that it was an artefact of diagenesis. They showed that in sulphur-rich dysoxic sediments, sulphurisation of organic matter during early diagenesis serves to preserve more of the labile OM fractions, particularly isotopically heavy carbohydrates ($\delta^{13}C$ of −16 to −22‰). These authors also noted that high amounts of labile OM may be delivered to marine sediments by increased terrestrial runoff, increased marine productivity, or a combination of both.

We investigated the relationship between $\delta^{13}C_{TOC}$, total sulphur (S) and indicators for anoxia (Mo) and marine productivity (Ba/Ti, U/Ti) in the Angora and mid-Waipara sections, which represent two contrasting lithotypes within Waipawa organofacies (Fig. 4). Significant positive correlations are observed between $\delta^{13}C_{TOC}$ and S (mid-Waipara: $r^2 = 0.71$, $n = 30$; Angora: $r^2 = 0.69$, $n = 24$). Positive correlations are also observed between $\delta^{13}C_{TOC}$ and the proxies for anoxia and productivity at mid-Waipara (Mo: $r^2 = 0.76$, Ba/Ti: $r^2 = 0.34$, U/Ti: $r^2 = 0.39$; $n = 30$). Some of the peaks in TOC at Angora correspond with peaks in U/Ti, but neither productivity proxy is correlated with $\delta^{13}C_{TOC}$. This may reflect a higher degree of diagenesis at Angora, due to greater burial and compressional tectonism within the East Coast Basin (Field et al., 1997), which may cause some overprinting or migration of geochemical signatures.

Palynology and biomarker analysis also help to identify the relationship between TOC and environmental changes at mid-Waipara (Fig. 4). A gradual increase in TOC from ~5 m below the base of the Waipawa organofacies parallels an increase in peridiniod dinocysts, which are thought to represent primarily heterotrophic dinoflagellates. There is also a general increase in terrestrial palynomorphs in the upper Waipara Greensand; pollen and spores dominate palynomorph assemblages (>70% of the assemblage) from ~15 m below the base of the Waipawa organofacies. A stronger correlation is evident between TOC and the BIT index ($r^2 = 0.45$, $n = 21$), which is a geochemical indicator of terrestrial input (see above). These correlated trends suggest that the increase in TOC in the upper Waipara Greensand was mainly due to a gradual increase in terrigenous input but was coupled with an increase in marine productivity.

The gradual increase in TOC and accompanying positive shift in $\delta^{13}C_{TOC}$ observed at Tawanui (Fig. 3c) warrants further consideration because it lies within a fining-upwards unit with a highly bioturbated and erosional base. There are three possible explanations for the progressive development of Waipawa organofacies characteristics in this unit. The unit may record the onset of organofacies deposition following an erosional event. However, the low TOC in the lower part of the section may also be explained by oxidation as a consequence of bioturbation. A third possibility, that the entire unit is a mass flow deposit with the OM being redeposited and concentrated in the upper finer-grained sediments, seems unlikely because it does not account for correlation between TOC and $\delta^{13}C_{TOC}$: if the OM was redeposited it should have a more uniform $\delta^{13}C_{TOC}$ signature.

We infer that Waipawa organofacies deposition occurred under conditions of moderate dysoxia associated with moderate to high marine productivity, which was at least partly a response to increased terrestrial OM input as shown by Schiøler et al. (2010). The correlation between $\delta^{13}C_{TOC}$, S and Mo indicates that dysoxic conditions during Waipawa organofacies deposition facilitated early diagenetic sulphurisation that could have preserved isotopically heavy carbohydrates, leading to a positive excursion in $\delta^{13}C_{TOC}$.

3.3. Timing of deposition

Precise dating of Waipawa organofacies deposition is complicated by several factors: unconformities, variation in the geochemical signature between sections, patchy distribution of fossils (especially calcareous nannofossils), poor age control for dinocyst bioevents, and scarcity of reliable paleomagnetic data. However, we have utilised available biostratigraphy and magnetostratigraphy to develop initial age models for the key sections. Dinocyst assemblages indicate that Waipawa organofacies can be correlated with an interval that extends from upper Zone NZDP7 to lower NZDP8 (Crouch et al., 2014). We use two primary events to identify this interval: the lowest occurrence (LO) of *Manumiella rotunda* (upper NZDP7) and the highest occurrence (HO) of *Deflandrea foveolata* (base of NZDP8). Respectively, these two events occur near the onset and near the top of organofacies deposition in the Angora and mid-Waipara sections (Fig. 3b, e). The LO of *M. rotunda* also occurs in lowermost Waipawa organofacies at Tawanui (Fig. 3c). Nannofossil biostratigraphy in the Angora section indicates that Waipawa organofacies deposition began near the base of nannofossil zone NP6 and ended within zone NP7 (Fig. 3b). At Tawanui, Waipawa organofacies is bracketed by Zone NP6 directly below and NP8 in the overlying Wanstead Formation (Fig. 3c). One sample within the organofacies is also dated as NP6. This implies that, although the base of the organofacies is highly burrowed, the hiatus between the unit and underlying Te Uri Member must have been relatively short-lived. These results also confirm that the base of the Waipawa organofacies is within NP6. This correlation is consistent with magnetostratigraphy at ODP Site 1172 where Waipawa organofacies deposition begins in uppermost Chron C26r and terminates at an unconformity either within or above Chron C26n (Fig. 3f). Limited magnetostratigraphic control for the mid-Waipara section (Lurcock, 2012) also indicates that Waipawa organofacies deposition began within a reversed polarity interval tentatively correlated with upper Chron C26r. The Paleogene dinocyst assemblages described from ODP Site 1172 (Bijl et al., 2013) lack reliable bioevents to enable subdivision of the Paleocene dinocyst zone

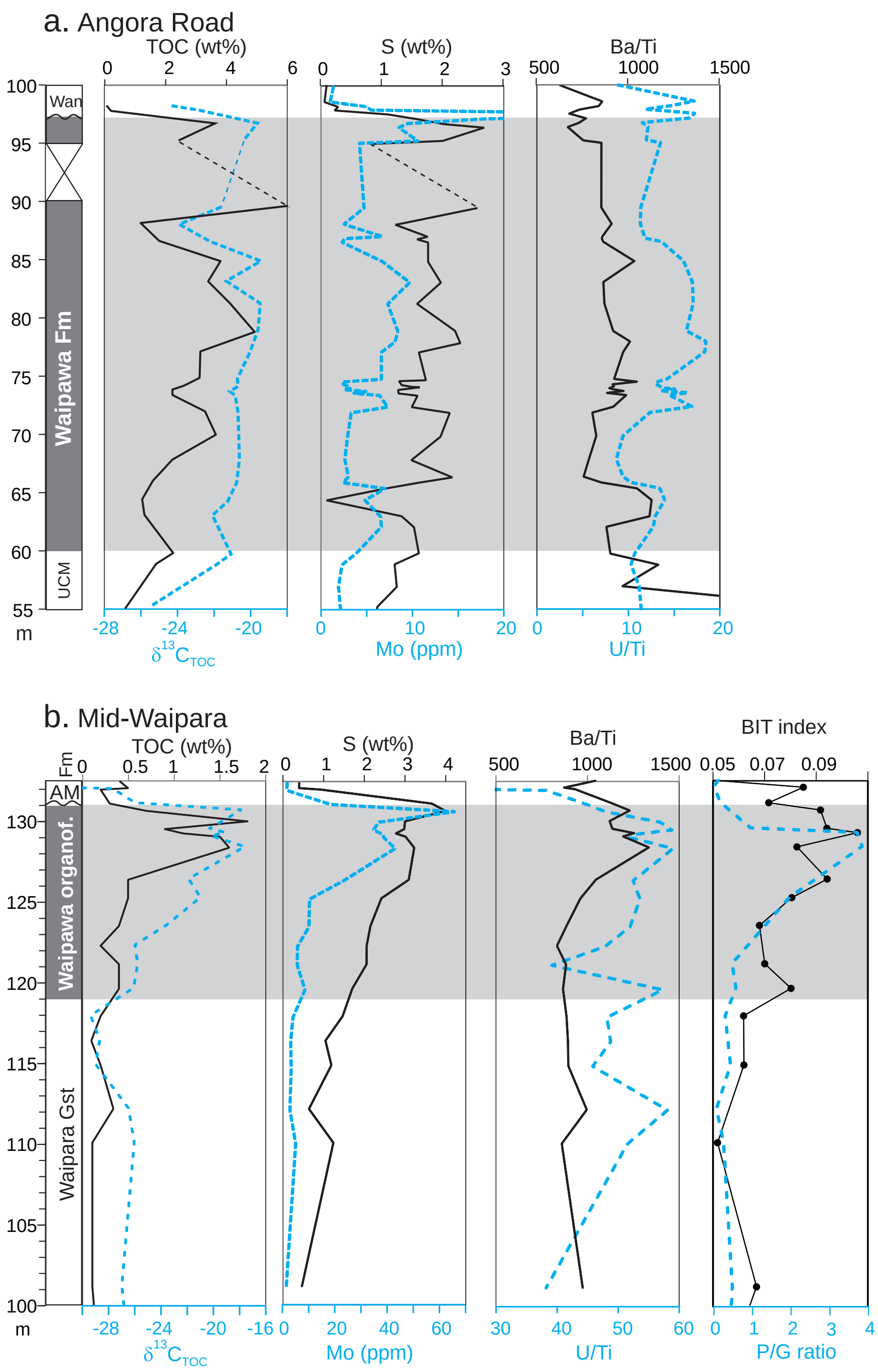

Fig. 4. Relationship between TOC, $\delta^{13}C_{TOC}$ and indicators for anoxia (S, Mo) and biological productivity (Ba/Ti, U/Ti) within the Waipawa organofacies in the (a) Angora Road and (b) mid-Waipara sections. Additional indicators of biological productivity (peridinioid/gonioaulicoid (P/G) ratio) and terrigenous input (BIT Index) are also shown for the mid-Waipara section.

(SPDZ1), and the species *D. foveolata* and *M. rotunda* were not recognised.

The biostratigraphic and magnetostratigraphic datums for the three most complete sections (Angora, mid-Waipara and ODP Site 1172) have been used to create age–depth plots (Fig. 5) according to the following conditions: (i) the line of correlation should lie above HOs and below LOs; (ii) nannofossil datums are well-constrained by age but not by stratigraphy as they occur sporadically in the sections; (iii) dinocyst datums are well-constrained by stratigraphy but not by age; (iv) the uppermost peak in organofacies characteristics is well-defined in all sections and is used as a tie point at 58.75 Ma. Crouch et al. (2014) placed the LO of *M. rotunda* at ~59 Ma. Our age-depth plots for the Angora and mid-Waipara sections (Fig. 5) allow us to confirm a date of 59.3 Ma for this datum. These plots indicate contrasting patterns of sedimentation. At Angora Road, an increase in sediment accumulation rate during Waipawa organofacies deposition (from 16 to 55 m/Ma) is consistent with the large increase in TOC (from ~0.75 to ~6 wt.%) being due to additional terrigenous input. At mid-Waipara, background sedimentation rates are similar to Angora but Waipawa organofacies deposition is not accompanied by an increase in accumulation rate. This is consistent with the smaller increase in TOC (from ~0.5 to ~1.75 wt.%), suggesting a smaller increase in terrigenous input. An increase in sediment

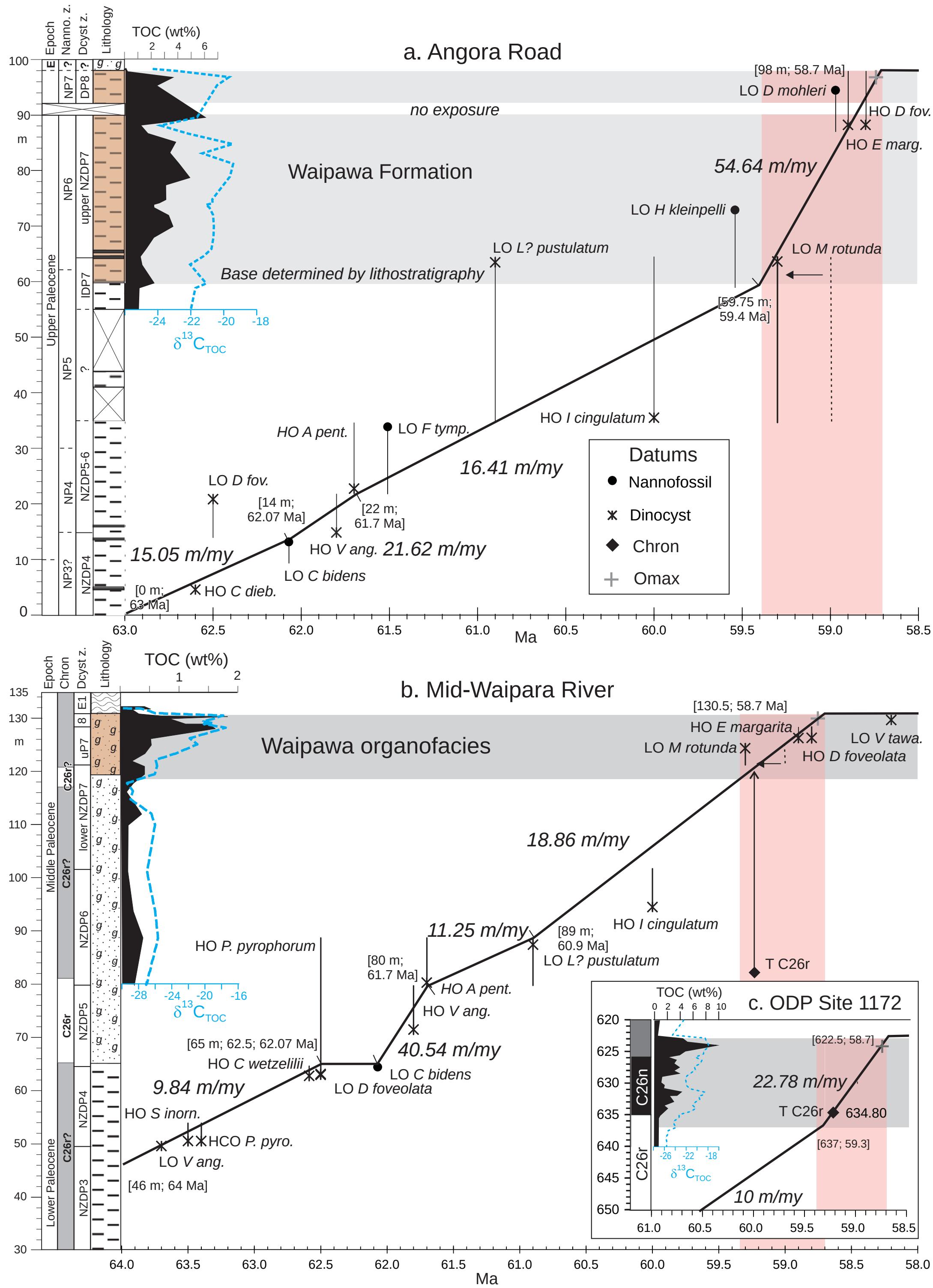

Fig. 5. Age depth plots for (a) Angora Road, (b) mid-Waipara River and (c) ODP Site 1172. Datums are listed in Supplementary Table S1; LO = lowest occurrence, HO = highest occurrence; Grey cross (+) = tie point based on upper maximum in $\delta^{13}C_{TOC}$. Vertical lines represent uncertainty between bounding samples. The line of correlation represents linear sediment accumulation rates (SAR) with a tick mark and label (depth; age) at each change in SAR.

accumulation rate at ODP Site 1172 is also consistent with the marked increase in TOC (Fig. 5).

Although these age models are relatively poorly constrained, there seems little reason to doubt that Waipawa organofacies deposition occurred as an isochronous event over a relatively short period of time (~700,000 years) in the late Middle to early Late Paleocene (59.4 to 58.7 Ma), spanning the Selandian–Thanetian Stage boundary.

3.4. Climatic cooling

It has been difficult to derive paleotemperature data from New Zealand Paleocene marine sediments that tend to be non-calcareous and sparsely fossiliferous, features that have also hampered biostratigraphic correlation (Hornibrook, 1992). Indeed, the absence of calcareous microfossils has been used to infer relatively cool water temperatures for the Paleocene (Jenkins, 1968). Similarly, the localised proliferation of diatoms and radiolarians on the Campbell Plateau and at Mead Stream has been used to infer cool conditions during the Late Paleocene (Hollis, 2002; Hollis et al., 2005a), either related to climatic cooling or enhanced upwelling of southern-sourced deep water. The abundance of siliceous microfossils in the pelagic sequence of eastern Marlborough has also been used to infer prolonged climatic cooling following the Cretaceous–Paleogene boundary event (Hollis, 2003). However, both approaches are qualitative and depend on uniformitarian assumptions.

GDGT-based temperature proxies provide a means to extract a paleotemperature record from carbonate-lean Paleocene marine sediments. In the mid-Waipara section, the TEX_{86} proxy has been used to derive sea surface temperature (SST) (Hollis et al., 2012) and the MBT′–CBT proxy has been used to derive mean annual air temperature (MAAT) (Pancost et al., 2013). The TEX^{L}_{86} calibration for SST indicates that deposition of Waipawa organofacies was associated with 2 °C of cooling from an average Paleocene SST of 15 °C to a minimum of ~13 °C in upper Waipawa organofacies (Fig. 6). Warmer average SSTs are indicated by the TEX^{H}_{86} calibration but the degree of cooling is greater (3 °C for a background SST of 21°). The paleo-calibration ($pTEX_{86}$) is used to assess which of these two modern calibrations provides the most robust guide to absolute SST values. As $pTEX_{86}$ values are significantly cooler than TEX^{H}_{86}, but within the calibration error of TEX^{L}_{86}, we conclude that TEX^{L}_{86} provides the best guide to SST changes at mid-Waipara and ODP Site 1172. The MBT′–CBT proxy also records minimum MAAT values in the upper Waipawa organofacies at mid-Waipara. The large calibration errors for the TEX^{L}_{86} and MBT′–CBT proxies (±4° and 4.9 °C, respectively) affect the absolute temperature estimates but not these trends in relative temperature. Significantly, both SST and MAAT proxies indicate that cooling began at the first positive shift in $\delta^{13}C_{TOC}$. This implies a close link between cooling and deposition of Waipawa organofacies.

Partly due to higher resolution sampling, the TEX_{86} record at ODP Site 1172 exhibits an even clearer relationship with Waipawa organofacies. The TEX^{L}_{86} calibration indicates that deposition of the organofacies was associated with cooling of almost 6 °C from a background temperature of 20 °C. The two peaks in $\delta^{13}C_{TOC}$ and TOC correspond to SST minima within this generally cool interval. Equivalent trends are seen in TEX^{H}_{86} and $pTEX_{86}$.

We have used the TEX_{86} proxy to investigate the SST trends through the deep marine Paleocene record at ODP Site 1121 on the eastern margin of the Campbell Plateau (Fig. 7). Sediments at this site span the interval of Waipawa organofacies deposition but its geochemical signature is not seen, presumably because of the deep-water setting. A lower bathyal–abyssal water depth is inferred for the Paleocene at Site 1121 whereas Waipawa organofacies deposition appears to have been restricted to mid-bathyal or shallower depths (Moore, 1988; Hollis et al., 2005a; Schiøler et al., 2010). An interval of reduced carbonate content is tentatively correlated with Waipawa organofacies because it is of equivalent age (Nannofossil zones NP6-7) and includes a zone of higher carbonate content and more negative $\delta^{13}C$ values as seen at Angora Road and Mead Stream (Fig. 3). GDGT recovery was too low to derive TEX_{86} values for the uppermost part of this interval. However, below this level, the proxy shows a clear cooling trend that parallels the decline in carbonate content. It is notable that offsets between the three TEX_{86} calibrations are different from those observed at mid-Waipara and ODP Site 1172. TEX^{L}_{86} and TEX^{H}_{86} values are generally in good agreement whereas $pTEX_{86}$ is significantly cooler. This tends to support the argument that GDGT distribution in sediments is strongly affected by water depth (Taylor et al., 2013). In this deep water site, agreement between the two standard calibrations indicates they are performing as observed in modern core-top studies (Kim et al., 2010). However, the cause of calibration offsets in the two samples that record coolest temperatures in TEX^{L}_{86} is uncertain. Consequently, we infer a relative cooling at ODP Site 1121 at the time of Waipawa organofacies deposition but cannot be certain of the magnitude of the cooling.

If we plot the data from Angora Road, mid-Waipara, ODP Site 1172 and ODP Site 1121 in the time domain (see Supplementary figure for

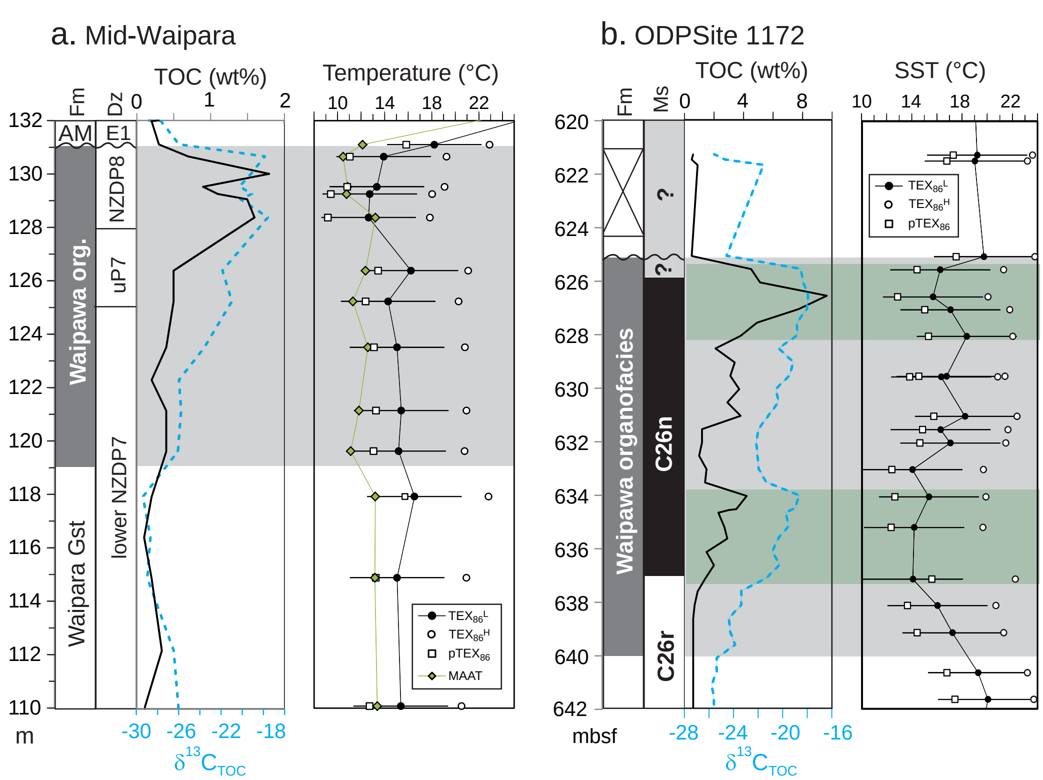

Fig. 6. Relationship between TOC, $\delta^{13}C_{TOC}$ and sea surface temperature (SST) derived from TEX^{L}_{86}, TEX^{H}_{86} and $pTEX_{86}$ for the mid-Waipara section and ODP Site 1172 (calibration error of ±4 °C is shown for TEX^{L}_{86}). Mean annual air temperature (MAAT) derived from the MBT′–CBT proxy is also shown for the mid-Waipara section (calibration error of ±4.9 °C).

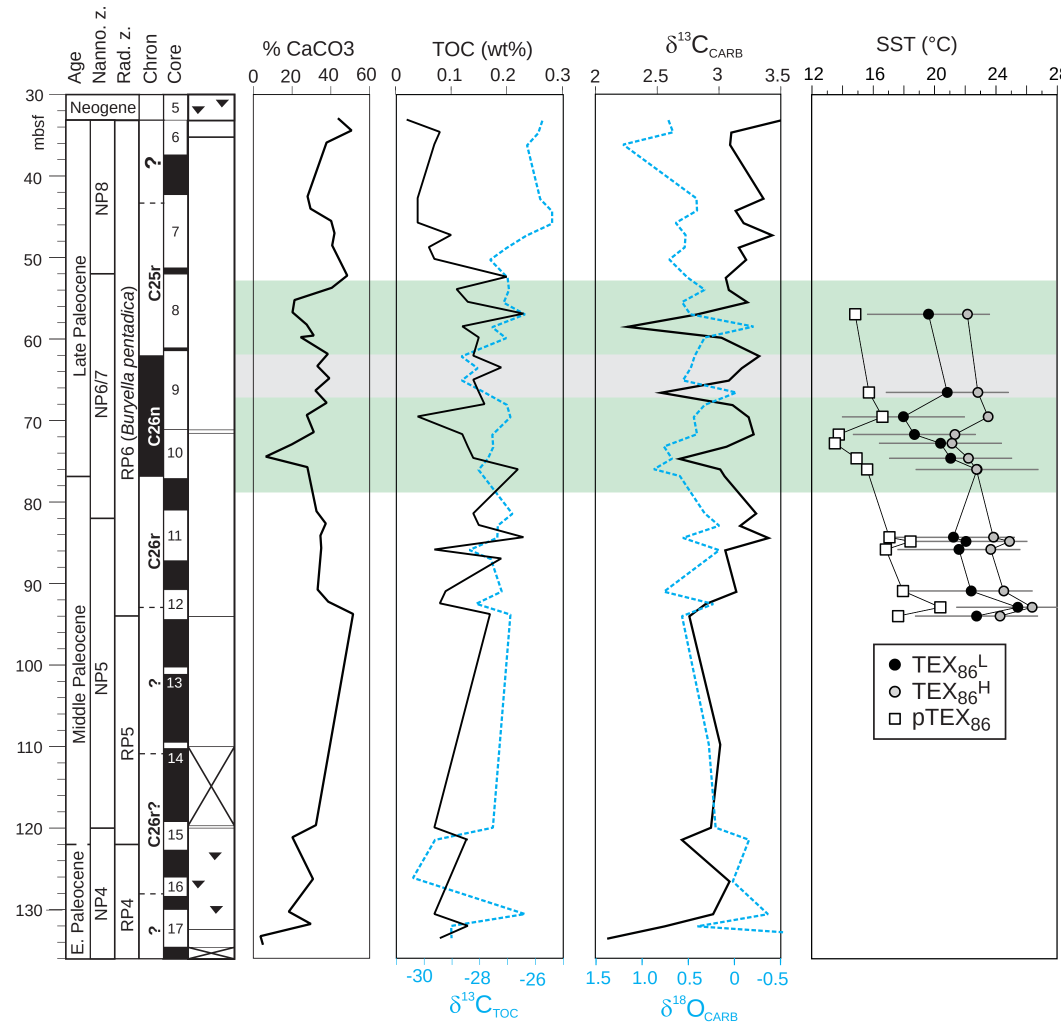

Fig. 7. Relationship between carbonate content (%CaCO3), TOC, $\delta^{13}C_{TOC}$, bulk carbonate $\delta^{13}C$ and $\delta^{18}O$, and sea surface temperature (SST) derived from TEX^L_{86}, TEX^H_{86} and $pTEX_{86}$ for ODP Site 1121 (calibration error of ±4 °C is shown for TEX^L_{86}).

age-depth plot for ODP Site 1121), we can examine the relationship between temperature and organofacies development in more detail (Fig. 8). The Angora section is too thermally mature to yield GDGT data, but provides a complementary record of Waipawa organofacies development, extending from ~59.4 to ~58.7 Ma. A weak cooling trend in SST and a distinct ~1.5 °C cooling step in MAAT is seen at the onset of organofacies deposition at mid-Waipara. Both proxies record ~2 °C cooling in the upper phase of Waipawa organofacies deposition, resulting in minimum values of 12.5 °C for SST and 10.5 °C for MAAT. Waipawa organofacies deposition is closely correlated with SST at ODP Site 1172. The initial positive shift in $\delta^{13}C_{TOC}$ is associated with pronounced cooling of 6 °C over 0.4 Myrs (from 20° to 14 °C). In contrast to mid-Waipara, SST is coldest (14 °C) in the lower peak in organofacies, warming by 4 °C within the organofacies trough and then cooling by 2 °C in the uppermost part of the upper peak.

The TEX_{86} record from ODP Site 1121 is problematic. It is hard to envisage a situation where oceanic SST is ~3 °C warmer than coastal SST at a lower latitude (Fig. 1), which is the case for Site 1121 and mid-Waipara when using the TEX^L_{86} calibration (Fig. 8). Although SSTs determined using the TEX^H_{86} calibration are in closer agreement between the three sites (Supplementary Figure S3), we have previously shown that the TEX_{86} calibration overestimates absolute temperature by >4 °C at mid-Waipara and ODP Site 1172 (Hollis et al., 2012). Moreover, the MAAT estimates support the use of the TEX^L_{86} calibration for absolute temperature reconstructions (Pancost et al., 2013). We are left to conclude that the close correspondence between TEX^L_{86} and TEX^H_{86}-based SSTs at Site 1121 is because *both* proxies are overestimating mean annual SSTs and $pTEX_{86}$ is the better guide to absolute mean annual temperature at this site. Certainly, SSTs derived from $pTEX_{86}$ for Site 1121 agree well with the TEX^L_{86}-based SST records from the other two sites, with a minimum SST of 13–14 °C at ~59.15 Ma (Fig. 8).

Offsets in the correlation of peaks and troughs between sections may be an artefact of the age model. Higher resolution data for the mid-Waipara and Angora sections may allow for tuning the three sections using tie points in the $\delta^{13}C$ or TOC records. Nevertheless, some general features of the temperature record appear to be genuine differences between proxies and records. Firstly, the ~2 °C offset between SST and MAAT at mid-Waipara is plausibly explained by a summer bias in the SST proxy (Hollis et al., 2012; Pancost et al., 2013). However, this implies that already cool conditions (MAAT of 13 °C) in the Middle Paleocene of mid-latitude (53°S) New Zealand cooled a further 2–3 °C during the coolest phases of Waipawa organofacies deposition (10–11 °C). These temperature estimates are no warmer than present day cool temperate southern New Zealand (MAAT of 11 °C at 45°S; NIWA climate database, cliflo.niwa.co.nz). Secondly, SSTs at ODP Site 1172 are ~2–4 °C warmer throughout the Paleocene apart from the interval spanning the lower organofacies peak (59.3–58.9 Ma). This implies that initial cooling may have caused westward expansion of a cool watermass that subsequently contracted for the remainder of the event. The final phase of the preserved cooling event appears to have

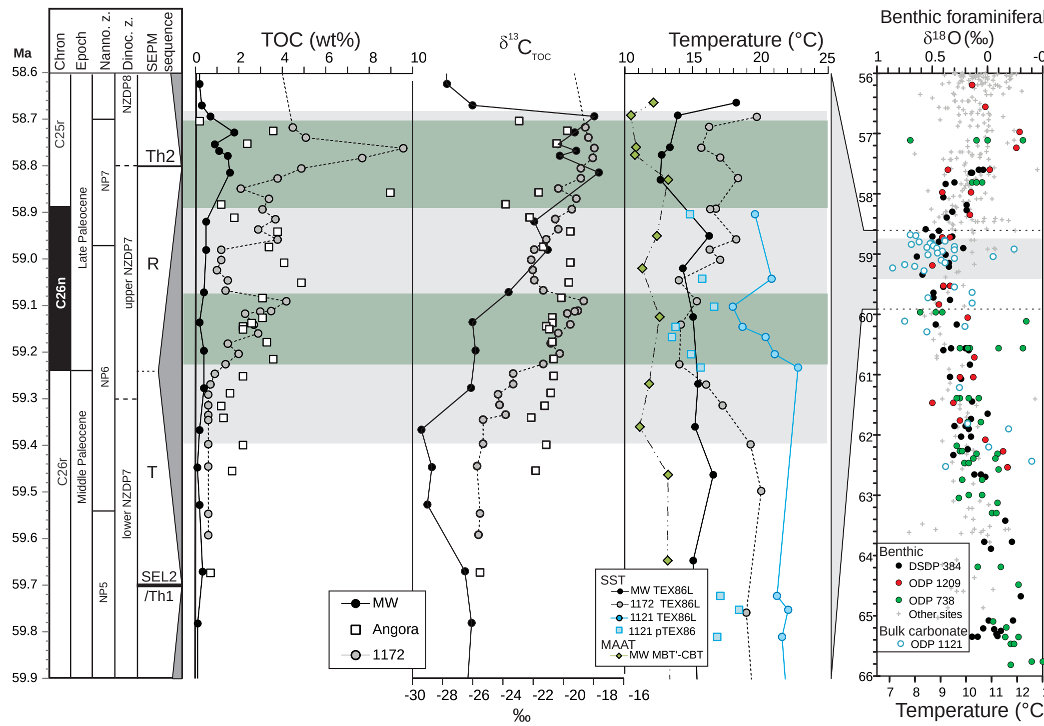

Fig. 8. Variation in TOC, $\delta^{13}C_{TOC}$ and temperature proxies plotted against age (59.9 to 58.6 Ma) for Angora Road, mid-Waipara, ODP Site 1172 and ODP Site 1121. The Light grey band represents distribution of Waipawa organofacies at the three sections. The two light green bands represent peaks in TOC and $\delta^{13}C_{TOC}$ and SST minima at Site 1172. Temperature estimates are derived from the TEX^{L}_{86} SST proxy and the MBT′–CBT MAAT proxy. Panel on right shows a global compilation of Paleocene $\delta^{18}O$ values from benthic foraminifera (Cramer et al., 2011 — with records from DSDP Site 384, ODP Site 738 and ODP Site 1209 highlighted) and the bulk carbonate $\delta^{18}O$ values for ODP Site 1121 (Wei et al., 2005). All records are recalibrated to GTS 2012.

been most pronounced in New Zealand, with equivalent effects on the land and in the ocean. Because erosion truncates the cooling event in all of these sections (Fig. 10), it is possible that further cooling occurred above the preserved record.

The regional cooling recorded in SW Pacific SST and MAAT proxies is correlated with the peak in a long-term positive excursion in the deep sea $\delta^{18}O$ (Fig. 8), which is well documented at north Atlantic DSDP Site 384 and at north Pacific ODP Site 1209 (Berggren et al., 2000; Westerhold et al., 2011). A positive $\delta^{18}O$ excursion of 0.8‰ represents a cooling of 4 °C or an 80 m fall in glacioeustatic sea level (Pekar et al., 2002).

Some additional lines of evidence support periodic but significant climatic cooling during the Paleocene. Kennedy (2003) used physiognomic analysis of leaf fossils for Paleocene sites in western and eastern South Island to infer a cool temperate climate with a mean annual air temperature (MAAT) of 9–11 °C, which is consistent with the results from the MBT′–CBT proxy. Analysis of pollen assemblages from ODP Site 1172 also shows pronounced cooling from warm to cool temperate conditions coincident with Waipawa organofacies deposition, with MAAT of ~10 °C (Contreras et al., 2014).

Growth of Antarctic ice sheets and calving of icebergs have also been used to explain the occurrence of bands of lone-stones in the Paleocene Whangai Formation at Angora Road and Riversdale, coastal Wairarapa (Leckie et al., 1995). We have confirmed the Angora Road occurrence and found further lone-stones in the Waipawa Formation at this locality (Tayler, 2011). We have also found a comparable band of lone-stones near the top of the Garden Cove Formation on Campbell Island (Andrew, 2010). Although petrographic studies are so far inconclusive, it remains possible that these exotic clasts are ice-rafted drop-stones and record discrete ice-rafting episodes in the Paleocene (~64.5 Ma at Campbell Island, ~62 and 59.3 Ma at Angora Road).

The occurrence of Paleocene biosiliceous sediments at ODP Site 1121 and Mead Stream (Hollis, 2002; Hollis et al., 2005a), glauconitic condensed sections within the Paleocene pelagic sequence in other parts of eastern Marlborough and Kaikoura (Hollis et al., 2005b; Fig. 10), and a condensed phosphatised and biosiliceous Paleocene section on northern Chatham Island (Campbell et al., 1993) suggests cool water upwelling intensified in this region during the Middle and Late Paleocene. The radiolarian assemblages in sediments of this age at ODP Site 1121 contain abundant *Cycladophora* (Hollis, 2002), a genus typical of cool water masses in the Cenozoic (Lombari and Lazarus, 1988).

3.5. Related climatic and biotic events

The onset of Waipawa organofacies deposition appears to have occurred at the same time as a short-lived enigmatic event, termed the Early–Late Paleocene biotic event (ELPE) or mid-Paleocene biotic event (MPBE), which is reported in central Pacific and south Atlantic ODP sites (Hancock and Dickens, 2005; Petrizzo, 2005; Westerhold et al., 2008, 2011) and at Zumaia, northern Spain (Bernaola et al., 2007; Schmitz et al., 2011). This short-lived (~50 kyr) biotic turnover event occurs at the top of Chron C26r within nannofossil zone NP6, directly below the Middle–Late Paleocene boundary (Fig. 10). Although the event has some similarities with biotic turnover events during hyperthermals, such as the Paleocene–Eocene Thermal Maximum (PETM), only the record at Zumaia shows evidence for warming associated with a negative $\delta^{13}C$ excursion. In central Pacific deep sea cores, the ELPE is a condensed interval characterised by carbonate dissolution (Hancock and Dickens, 2005; Petrizzo, 2005). It does not appear to be associated with negative excursions in either $\delta^{18}O$ or $\delta^{13}C$ in central Pacific ODP Site 1209. However, Westerhold et al. (2011) suggest that this is an artefact of dissolution as $CaCO_3$ concentration falls to ~65 wt.% (Hancock and Dickens, 2005). Significantly, the ELPE marks the base of an extended interval of maximum $\delta^{13}C$ (>1.5‰) at this site, which is correlated with the Paleocene carbon isotope maximum (PCIM) (Shackleton, 1986; Corfield and Cartlidge, 1992; Thompson and Schmitz, 1997; Hollis et al., 2005a). At Site 1209, the ELPE is also located within the extended interval of relatively positive $\delta^{18}O$ values noted above (Westerhold et al., 2011).

3.6. Sea level changes

The early Paleogene is commonly considered to have been "ice-free" (Zachos et al., 2001, 2008) because there is little direct evidence for the presence of polar ice sheets prior to the Late Eocene. However, broad-scale correlation of unconformities across geographic regions and the general correspondence between global sea-level reconstructions and the deep-sea oxygen isotope record through the Late Cretaceous and early Paleogene has been taken as evidence that small ice sheets waxed and waned through this time period (e.g. Rhodes et al., 1999; Miller et al., 2005; Crampton et al., 2006; Browning et al., 2008; Harris et al., 2010; Cramer et al., 2011; Miller et al., 2011). Moreover, recent geophysical models suggest that Antarctica may have had sufficiently high elevation for substantial ice sheets to form in upland areas during cool episodes within the early Paleogene (Wilson and Luyendyk, 2009; Wilson et al., 2013).

When reconstructing sea-level change from sedimentary records across the globe we need to take into account the influences of: (i) regional basin subsidence changes (ii) regional isostatic adjustments due to the redistributions of mass as a result of sea level change and ice buildup and (iii) the effect of self-gravitation that the newly formed Antarctic glaciers have on regional Southern Hemisphere sea-level change. All of these effects are strongly dependent on the locus of ice sheet formation. Moreover, the expression of the resulting regional sea-level change is strongly dependent on the regional thickness of the lithosphere, i.e., the 'flexibility' of the local lithosphere to respond to the forcing. For instance, it has been shown from the combination of regional sea-level reconstructions around Antarctica and numerical modelling that during the Eocene–Oligocene continental ice expansion on Antarctica, regional Southern Ocean sea level rose by up to more than two times the predicted eustatic sea-level fall (Stocchi et al., 2013). If the primary locus for ice formation was East Antarctica in late Paleogene, these three factors are inferred to have been counterbalanced at the latitude of ~60–65°S. Further north, sea-level fall is predicted to have been greater than the eustatic (global average), although still subject on regional paleogeographic controls. Paleogene New Zealand was situated within the range of latitudes for which a eustatic sea-level fall is a reasonable estimate, albeit with local variation due to proximity to the locus of ice accumulation and lithosphere thickness.

Four lines of evidence indicate that typical Waipawa organofacies was deposited during a regional fall in sea level: (i) foraminiferal assemblages indicate that paleodepth shallows from middle to outer shelf in the underlying unit to inner shelf within Waipawa organofacies, both in the East Coast Basin (Moore, 1988) and Great South Basin (Cook et al., 1999; Schiøler et al., 2010); (ii) palynofacies record an increase in terrestrial OM, consistent with closer proximity to the shoreline in East Coast, Canterbury and Great South Basins (Schiøler et al., 2010); (iii) the distribution of the Tartan Formation in the Great South Basin is consistent with a fall in base level, with deposition in the deepest parts of the basin and erosion or non-deposition in shoreward parts of the basin (Schiøler et al., 2010); and (iv) the wide geographic extent of the equivalent facies, reported here from eastern New Zealand to the eastern margin of Tasmania (regions separated by an active spreading ridge), indicates that this is more likely to be a response to global changes in sea level rather than local tectonic uplift.

There is widespread evidence for a significant fall in relative sea level or a series of falls occurring within the latest Middle to early Late Paleocene. Waipawa deposition is most closely associated with the two falls in sea level represented by the Sel2/Th1 and Th2 sequence boundaries in the European Basin sequence (Haq et al., 1987; Hardenbol et al., 1998; Schmitz et al., 2011). These two sequences have been correlated with the New Jersey Coastal Plain succession, where they are named Pa2a and Pa2b (Browning et al., 2008; Kominz et al., 2008; Harris et al., 2010; Cramer et al., 2011). Estimates for the magnitude of sea-level fall associated with these sequences range from >50 m (Haq et al., 1987) to ~25 m (Kominz et al., 2008) to ~12–15 m (Harris et al., 2010; Cramer et al., 2011). A range value of 15–25 m would be sufficient to explain the changes in palynofacies and foraminiferal assemblages observed in the East Coast and Great South Basins.

Sequence stratigraphic interpretation of Waipawa organofacies deposition is complicated by the recognition of two distinct depositional motifs. Typical Waipawa organofacies deposition, as seen at Angora Road, is consistent with a regressive motif and comprises a coarsening upwards sequence capped by an unconformity. Similar patterns are evident at mid-Waipara and ODP Site 1172. In other sections, Waipawa organofacies is deposited above a sharp contact that is either a possible unconformity (Mead Stream) or an obvious unconformity with an intensely burrowed contact (Tawanui). The base of the unit at Mead Stream is correlated with a regional unconformity overlain by glauconitic sandstone in sections closer to the paleo-shoreline, notably at Muzzle and Bluff Streams in the middle Clarence valley (Hollis et al., 2005b) and Kaikoura Peninsula (Rattenbury et al., 2006). Thus, Waipawa organofacies appears to occur at the base of a fining-upwards transgressive motif at Mead Stream and Tawanui: greensand or siliceous mudstone grading up into calcareous mudstone or micrite. These two opposing motifs (coarsening-up and capped by unconformity, and fining-up above an unconformity) are likely to be the result of localised variations in accommodation space: the regressive motif occurs where subsidence and sedimentation rates were high and the transgressive motif occurs where subsidence and sedimentation rates were low. Our sequence stratigraphic model (Fig. 9) reconciles these two motifs and also accounts for the two phases of Waipawa organofacies deposition that are represented by two distinct units at Mead Stream and two intervals of peak TOC and $\delta^{13}C$ at Angora Road and ODP Site 1172. We suggest that Waipawa organofacies was deposited during two regressive–transgressive cycles that are uncertainly correlated with the Sel/Th1-Th2 sequences.

The transgression that follows Waipawa organofacies deposition continued through the Paleocene–Eocene transition, into the late Early Eocene (King et al., 1999). This regional sea-level record is consistent with the long-term Northern Hemisphere sea-level record (Haq et al.,

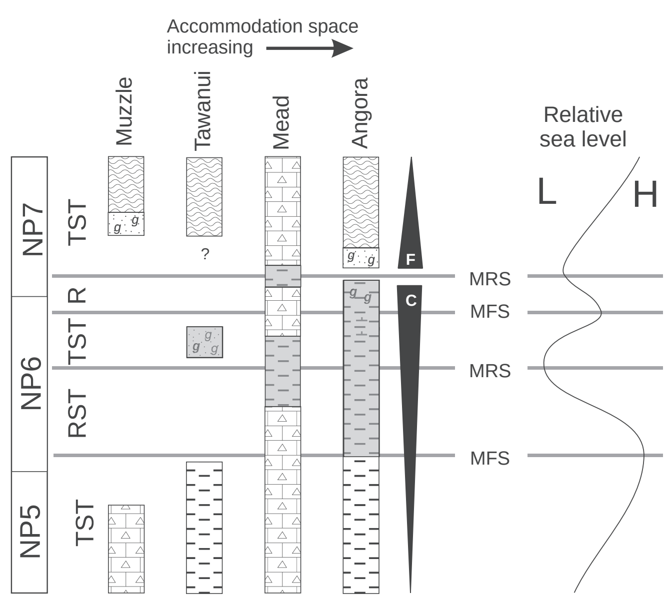

Fig. 9. A sequence stratigraphic model for Waipawa organofacies (shaded grey) deposition across two regressive-transgressive cycles. TST, transgressive systems tract; RST, regressive systems tract; L, low; H, high; MFS = maximum flooding surface; MRS = maximum regressive surface (nomenclature follows Catuneanu, 2006).

1987; Hardenbol et al., 1998; Miller et al., 2005, 2011; Cramer et al., 2011) in which the sea-level fall in earliest, Late Paleocene (~59 Ma) is succeeded by prolonged transgression that peaked in the late, Early Eocene (~52 Ma).

3.7. Regional unconformity

One of the defining features of large-scale Antarctic glaciation in the Early Oligocene is the development of a major regional unconformity, the Marshall Unconformity or Paraconformity (Carter, 1985; Fulthorpe et al., 1996; Nelson and Cooke, 2001; Carter et al., 2004), which occurs throughout the Southwest Pacific. The combined effects of erosion due to a fall in base level and scour and non-deposition due to intensified flows of southern sourced currents is an hiatus that is centred on the Oi2 glaciation (Miller et al., 1991) in the Early Oligocene, but in some settings may extend over much of the Cenozoic. One example is ODP Site 1121, on the eastern margin of the Campbell Plateau, where Paleocene drift sediments are overlain by a thin veneer of ferromanganese nodule-bearing sediments of late Neogene age (Graham et al., 2004).

A closely comparable unconformity is associated with Late Paleocene cooling (Fig. 10). The unconformity records maximum regression at the top of the Waipawa organofacies in settings where both sedimentation and subsidence rates were high (e.g. Angora, mid-Waipara, ODP Site 1172). In settings where sedimentation rates were lower (e.g. Tawanui), erosion has removed the regression-related Waipawa organofacies sediments and, instead, the transgressive motif of Waipawa organofacies is present above an unconformity. At Tawanui, the transgressive phase is well expressed with an intensely burrowed unconformity overlain by a dark greensand unit that contains somewhat depleted geochemical features of the Waipawa organofacies. In other localities, such as Muzzle Stream in Clarence valley, more time is missing and the unconformity has eroded every remnant of the Waipawa organofacies. Instead, a highly burrowed surface is overlain by a greensand unit, the Teredo Limestone, the basal member of the Amuri Limestone (Reay, 1993). At Muzzle Stream, Teredo Limestone is of Late Paleocene age and grades up into the Lower Limestone Member of the Amuri Limestone (Hollis et al., 2005b). A few km to the south and closer to the paleo-shoreline at Bluff Stream, the unit is of Early Eocene age and is overlain by a thinner Lower Limestone Member succession, which grades into Lower Marl Member (Hollis et al., 2005b). A similar sequence is observed on Kaikoura Peninsula (Fig. 10), which may have been even closer to the paleo-shoreline (Crampton et al., 2003). Although these sites are closer to the paleo-shoreline than Mead Stream, the background pelagic facies suggest at least outermost shelf to upper bathyal water depths (Hollis et al., 2005a, b). Thus, erosion at the base of the Teredo Limestone is considered to be due to intensification of currents and deep-sea scour rather than a direct effect of sea-level fall.

The Middle–Late Paleocene unconformity can be traced further afield although it is often overprinted by the Eocene–Oligocene Marshall Unconformity. The northernmost record we have identified in eastern New Zealand is at Mangahouanga Stream, northern Hawke's Bay (Fig. 2) (Moore, 1987, 1988; Wilson and Moore, 1988; Supplementary Figure S1). The section is only a few km from the Te Hoe River section, but contains no vestige of the Waipawa Formation. Instead, Paleocene Whangai Formation is unconformably overlain by Paleocene–Eocene Wanstead Formation (Wilson and Moore, 1988).

To the northwest of New Zealand, the Paleocene unconformity is present in Paleogene DSDP cores on the Lord Howe Rise (Figs. 1, 2). The unconformity truncates Middle Paleocene pelagic strata at DSDP Sites 206, 207 and 208, with the age of overlying sediments younging to the northwest: Late Paleocene at Site 207, Early Eocene at Site 206 and Middle Eocene at Site 208 (Burns et al., 1973; Edwards, 1973). Because these sediments were deposited at bathyal depths, erosion was probably caused by scour of northwest-flowing bottom currents (Fig. 1b).

To the south of New Zealand the unconformity is recorded in the Great South Basin (Schiøler et al., 2010), on Campbell Island (Beggs, 1978; Hollis et al., 1997b) and at DSDP Site 277 on the western Campbell Plateau (Fig. 10) (Hollis et al., 1997b). On Campbell Island, the unconformity is a sharp contact between Cretaceous–Paleocene Garden Cove Formation and Eocene–Oligocene Tucker Cove Formation. The unconformity is well exposed at Limestone Point, Northwest Bay, and at Camp Cove (Hollis et al., 1997). Dinocyst biostratigraphy and magnetostratigraphy indicate that the uppermost Garden Cove Formation is middle Early Paleocene age (Fig. 10). As the base of the overlying Tucker Cove Formation is late Early Eocene age, the unconformity represents a hiatus of ~13 million years. At DSDP Site 277, a shorter hiatus of ~2 m.y. (~59–57 Ma) has been identified by nannofossil biostratigraphy (Supplementary Table S3).

3.8. Conditions for Antarctic glaciation

The Paleocene stratigraphy of the Southwest Pacific contains convincing evidence that a regional sea-level fall coincided with increased scour by bottom currents on submarine highs and significant cooling on land and in the oceans over a period of 700 kyrs (Fig. 10). Cooling appears to have occurred in two pulses separated by ~400 kyrs. Cooling and sea-level fall at this level of periodicity is typical of glacioeustasy (Miller et al., 2005). Growth or expansion of an Antarctic ice sheet is not essential for intensification of deep-water formation but it seems a plausible cause for a short-lived increase in the strength of bottom currents sweeping north along the eastern and western margins of New Zealand and causing erosion from the Campbell Plateau to the Lord Howe Rise (Fig. 1b). Although there is no direct lithological evidence for glaciation in the early Paleogene, the absence of glacial sediments can be plausibly explained by ice sheets being restricted to upland areas (Wilson and Luyendyk, 2009; Wilson et al., 2013). Modelling based on these new reconstructions of Antarctic paleogeography has shown that permafrost may have waxed and waned through the Early Eocene, contributing to the carbon cycle changes that resulted in short-lived episodes of extreme warmth, such as the PETM (DeConto et al., 2012). In a climate regime significantly cooler than background conditions of the latest Paleocene and Early Eocene, it seems likely that permafrost would have been covered by ice sheets in the upland parts of Antarctica.

3.9. Accumulation of organic sediments

Perhaps the most challenging conundrum in interpreting Waipawa organofacies is to identify the features of the regional environment and global climatic trends that led to a truly unique depositional event. The distinctive features of this organofacies have not been recorded in any other time interval within the geological history of the Southwest Pacific. The correlation of TOC and $\delta^{13}C_{TOC}$ is plausibly explained by conditions of preservation associated with enhanced marine productivity and some degree of dysoxia (Sinninghe Damsté et al., 1998). Marine productivity is likely to have increased as a consequence of climatic cooling, which would intensify currents from the south and increase regional upwelling. But how does one account for the accompanying increase in terrestrial organic matter described by Schiøler et al. (2010)? A fall in base level will lead to greater coastal erosion. However, there is little evidence from other regressive events, such as at the Eocene–Oligocene transition or during Quaternary glaciations, that elevated coastal erosion is coupled with increased deposition of terrestrial organic matter. Indeed, the next regional episode of increased terrestrial carbon burial to follow this Paleocene event was a consequence of extreme global warming at the Paleocene–Eocene thermal maximum (Crouch et al., 2003), with similar episodes inferred for the

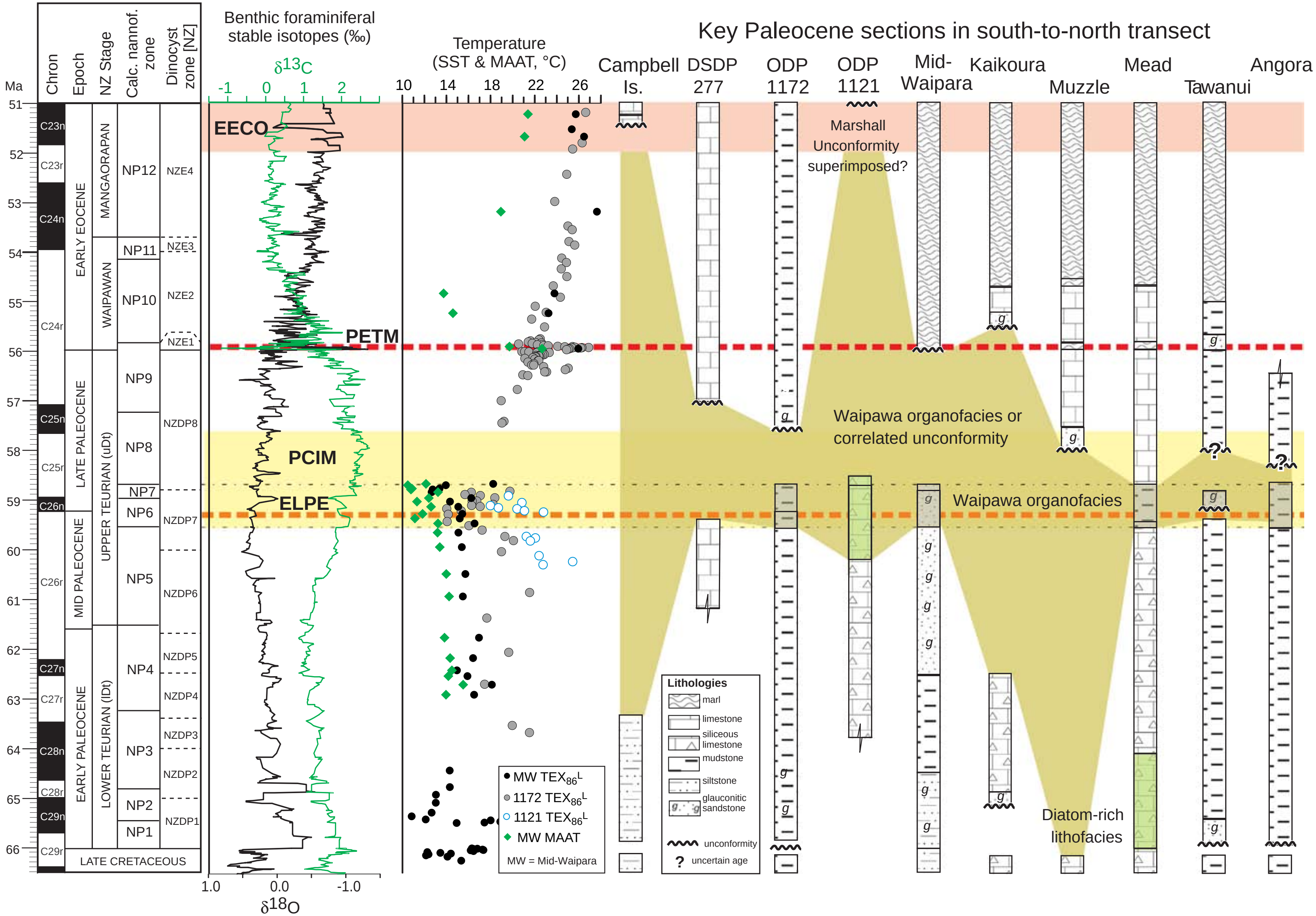

Fig. 10. Chronostratigraphy of Waipawa organofacies deposition, associated unconformities and trends in deep sea stable isotopes (Cramer et al., 2009, 2011) and regional temperatures (Bijl et al., 2009; Hollis et al., 2009; Sluijs et al., 2011; Hollis et al., 2012; Pancost et al., 2013).

subsequent Eocene hyperthermals (Nicolo et al., 2007; Slotnick et al., 2012).

We suggest that a unique set of circumstances led to Waipawa organofacies deposition:

(i) Mild temperatures through the Middle Paleocene (Fig. 10), promoted regional proliferation of coastal vegetation under warm temperate to cool subtropical conditions (Crouch et al., 2003; Contreras et al., 2014);
(ii) Tasman Sea-related extension slowed in the Late Paleocene, resulting in accelerated, passive thermal subsidence in sedimentary basins around New Zealand (King et al., 1999);
(iii) Pronounced and short-lived cooling at the Middle–Late Paleocene boundary, elevated nutrient supplies from both erosion of well-vegetated coastal areas and enhanced current-driven upwelling resulting in increased carbon delivery and burial;
(iv) A latest Paleocene to Early Eocene transgression linked to global warming (Sluijs et al., 2008), and passive margin subsidence led to deposition of fine-grained smectitic sediments (Field et al., 1997), preserving the underlying organofacies.

4. Conclusions

The Waipawa organofacies has been identified throughout the southwest Pacific, from the sedimentary basins of eastern New Zealand to the East Tasman Plateau, and at least as far north as the North Slope Basin (Fig. 1). It is present in sedimentary successions deposited at upper bathyal (Mead Stream) to inner shelf (Great South Basin) depths and records mass erosion and deposition of terrigenous sediments with abundant plant matter and rich in nutrients, which in some settings promoted high marine productivity and the development of dysoxic conditions. Deposition of this facies appears unique to this region. We suggest that a combination of regional tectonic and global climate trends may explain the widespread deposition of organic-rich sediments during a time of climate cooling.

The short-lived but pronounced regressive episode that led to deposition of Waipawa organofacies is associated with climatic cooling and deep-sea scour locally and a global fall in sea level. The coupling of sea-level fall and climatic cooling implies a glacio-eustatic driver for sea-level change prior to large-scale glaciation of polar regions in the Oligocene. This evidence for Paleocene glaciation supports other lines of evidence that indicate that circum-polar gateways were not the primary prerequisite for ice sheet growth on Antarctica (DeConto and Pollard, 2003; Barker and Thomas, 2004; Stickley et al., 2004; Pagani et al., 2011; Gasson et al, 2013).

The cause of glaciation at ~59 Ma is uncertain. The event lies near the onset of the PCIM, a time that is associated with high net carbon burial and low atmospheric CO_2 (Komar et al., 2013). It has been suggested that the PCIM signals recovery of the ocean ecosystem following extinctions and trophic collapse at the Cretaceous–Paleogene boundary: enrichment in ^{13}C indicating a general increase in biological production and carbon burial (Corfield and Norris, 1996; Norris et al., 2001). The resulting drawdown of atmospheric CO_2 may have led to global cooling and Antarctic glaciation.

Supplementary data to this article can be found online at http://dx.doi.org/10.1016/j.earscirev.2014.03.006.

Acknowledgments

We thank Sonja Fry, Randall McDonnell, Karyne Rogers, Marianna Terezow and Roger Tremain (all GNS Science) for technical assistance; Graeme Wilson for dinocyst data for Te Hoe River; GNS colleagues, Dominic Strogen and Kyle Bland provided helpful advice on stratigraphy. This research used samples and data provided by the Integrated Ocean Drilling Program (IODP). Funding for this research was provided by the New Zealand Marsden Fund and the GNS Global Change through Time Programme. PKB acknowledges funding from the Netherlands Organisation for Scientific Research (NWO — VENI Grant No. 863.13.002).

References

Andrew, B., 2010. Sedimentary facies and unconformity analysis of some Paleocene–Eocene sections, Marlborough and Campbell Island, New Zealand, MSc Thesis, Earth and Ocean Sciences. University of Waikato, Hamilton (227 pp.).
Barclay, R.S., McElwain, J.C., Sageman, B.B., 2010. Carbon sequestration activated by a volcanic CO_2 pulse during Ocean Anoxic Event 2. Nat. Geosci. 3, 205–208.
Barker, P.F., Thomas, E., 2004. Origin, signature and palaeoclimatic influence of the Antarctic Circumpolar Current. Earth Sci. Rev. 66, 143–162.
Beggs, J.M., 1978. Geology of the metamorphic basement and Late Cretaceous to Oligocene sedimentary sequence of Campbell Island, southwest Pacific Ocean. J. R. Soc. N. Z. 8, 161–177.
Bernaola, G., Baceta, J.I., Orue-Etxebarria, X., Alegret, L., MartÃ-n-Rubio, M., Arostegui, J., DinarÃ¨s-Turell, J., 2007. Evidence of an abrupt environmental disruption during the mid-Paleocene biotic event (Zumaia section, western Pyrenees). Geol. Soc. Am. Bull. 119, 785–795.
Bijl, P.K., Schouten, S., Sluijs, A., Reichart, G.-J., Zachos, J.C., Brinkhuis, H., 2009. Early Palaeogene temperature evolution of the southwest Pacific Ocean. Nature 461, 776–779.
Bijl, P.K., Houben, A.J.P., Schouten, S., Bohaty, S.M., Sluijs, A., Reichart, G.-J., Sinninghe Damste, J.S., Brinkhuis, H., 2010. Transient Middle Eocene atmospheric CO_2 and temperature variations. Science 330, 819–821.
Bijl, P.K., Sluijs, A., Brinkhuis, H., 2013. A magneto- and chemostratigraphically calibrated dinoflagellate cyst zonation of the early Palaeogene South Pacific Ocean. Earth Sci. Rev. 124, 1–31.
Browning, J.V., Miller, K.G., Sugarman, P.J., Kominz, M.A., McLaughlin, P.P., Kulpecz, A.A., Feigenson, M.D., 2008. 100 Myr record of sequences, sedimentary facies and sea level change from Ocean Drilling Program onshore coreholes, US Mid-Atlantic coastal plain. Basin Res. 20, 227–248.
Burns, R.E., Andrews, J.E., Van der Lingen, G.J., 1973. Initial Reports of the Deep Sea Drilling Project vol 21. US Govt, Printing Office, Washington, DC.
Campbell, H.J., Andrews, P.B., Beu, A.G., Maxwell, P.A., Edwards, A.R., Laird, M.G., Hornibrook, N.d.B., Mildenhall, D.C., Watters, W.A., Buckeridge, J.S., Lee, D.E., Strong, C.P., Wilson, G.J., Hayward, B.W., 1993. Cretaceous-Cenozoic geology and biostratigraphy of the Chatham Islands, New Zealand. Institute of Geological and Nuclear Sciences monograph 2, 1–269.
Cande, S.C., Stock, J.M., 2004. Cenozoic reconstructions of the Australia–New Zealand–South Pacific sector of Antarctica. In: Exon, N., Kennett, J.P., Malone, M. (Eds.), The Cenozoic Southern Ocean. AGU Geophysical Monograph, Washington DC, USA, pp. 5–18.
Carter, R.M., 1985. The mid-Oligocene Marshall Paraconformity, New Zealand: coincidence with global eustatic fall or rise? J. Geol. 93, 359–371.
Carter, R.M., McCave, I.N., Richter, C., et al., 1999. Proceedings of the Ocean Drilling Program, initial reports, volume 181: Southwest Pacific gateways, Sites, pp. 1119–1125.
Carter, L., Carter, R.M., McCave, I.N., 2004. Evolution of the sedimentary system beneath the deep Pacific inflow off eastern New Zealand. Mar. Geol. 205 (1–4), 9–27.
Catuneanu, O., 2006. Principles of Sequence Stratigraphy. Elsevier, Amsterdam.
Contreras, L., Pross, J., Bijl, P.K., O'Hara, R.B., Raine, J.I., Sluijs, A., Brinkhuis, H., 2014. Southern high-latitude terrestrial climate change during the Paleocene–Eocene derived from a marine pollen record (ODP Site 1172, East Tasman Plateau). Clim. Past Discuss. 10, 291–340.
Cook, R.A., Sutherland, R., Zhu, H., 1999. Cretaceous–Cenozoic geology and petroleum systems of the Great South Basin, New Zealand. 20 (190 pp.).
Corfield, R.M., Cartlidge, J.E., 1992. Oceanographic and climatic implications of the Palaeocene carbon isotope maximum. Terra Nova 4, 443–455.
Corfield, R.M., Norris, R.D., 1996. Deep water circulation in the Paleocene ocean. In: Knox, R.W.O.B., Corfield, R.M., Dunay, R.E. (Eds.), Correlation of the Early Paleogene in Northwest Europe. Geological Society Special Publication No. 101, pp. 443–456.
Cramer, B.S., Toggweiler, J.R., Wright, J.D., Katz, M.E., Miller, K.G., 2009. Ocean overturning since the Late Cretaceous: inferences from a new benthic foraminiferal isotope compilation. Paleoceanography 24, PA4216.
Cramer, B.S., Miller, K.G., Barrett, P.J., Wright, J.D., 2011. Late Cretaceous–Neogene trends in deep ocean temperature and continental ice volume: reconciling records of benthic foraminiferal geochemistry ($\delta^{18}O$ and Mg/Ca) with sea level history. J. Geophys. Res. 116, C12023.
Crampton, J., Laird, M., Nicol, A., Townsend, D., Van Dissen, R., 2003. Palinspastic reconstructions of southeastern Marlborough, New Zealand, for Late Cretaceous to Eocene times. N. Z. J. Geol. Geophys. 46, 153–175.
Crampton, J.S., Schiøeler, P., Roncaglia, L., 2006. Detection of Late Cretaceous eustatic signatures using quantitative biostratigraphy. Geol. Soc. Am. Bull. 118, 975–990.
Crouch, E.M., Brinkhuis, H., Visscher, H., Crouch, E.M., Hollis, C.J., Rogers, K.M., Dickens, G. R., Dickens, G.R., Aubry, M.P., 2003. The *Apectodinium* acme and terrestrial discharge during the Paleocene–Eocene thermal maximum: New palynological, geochemical and calcareous nannoplankton observations at Tawanui, New Zealand. Palaeogeogr. Palaeoclimatol. Palaeoecol. 194, 387–403.
Crouch, E.M., Willumsen, P.S., Kulhanek, D.K., Gibbs, S.J., 2014. A revised Paleocene (Teurian) dinoflagellate cyst zonation from eastern New Zealand. Rev. Palaeobot. Palynol. 202, 47–79.
DeConto, R.M., Pollard, D., 2003. Rapid Cenozoic glaciation of Antarctica induced by declining atmospheric CO_2. Nature 421, 245–249.

DeConto, R.M., Galeotti, S., Pagani, M., Tracy, D., Schaefer, K., Zhang, T., Pollard, D., Beerling, D.J., 2012. Past extreme warming events linked to massive carbon release from thawing permafrost. Nature 484, 87–91.

Edwards, A.R., 1973. Southwest Pacific regional unconformities encountered during Leg 21. Initial Rep. Deep Sea Drill. Proj. 21, 701–720.

Exon, N.F., Kennett, J.P., Malone, M.J., et al., 2001. Proceedings, ODP Initial Reports, Leg 189. Ocean Drilling Program, College Station, TX.

Field, B.D., Uruski, C.I., et al., 1997. Cretaceous–Cenozoic geology and petroleum systems of the East Coast Region. Institute of Geological and Nuclear Sciences Monography. 19 (301 pp.).

Fulthorpe, C.S., Carter, R.M., Miller, K.G., Wilson, J., 1996. Marshall Paraconformity: a mid-Oligocene record of inception of the Antarctic Circumpolar Current and coeval glacio-eustatic lowstand? Mar. Pet. Geol. 13 (1), 61–77.

Gasson, E., Lunt, D.J., DeConto, R., Goldner, A., Heinemann, M., Huber, M., LeGrande, A.N., Pollard, D., Sagoo, N., Siddall, M., Winguth, A., 2013. Uncertainties in the modelled CO_2 threshold for Antarctic glaciation. Clim. Past Discuss. 9, 5701–5745.

Gradstein, F.M., Ogg, J.G., Schmitz, M., Ogg, G., 2012. The Geologic Time Scale. Elsevier, Amsterdam.

Graham, I.J., Carter, R.M., Ditchburn, R.G., Zondervan, A., 2004. Chronostratigraphy of ODP 181, Site 1121 sediment core (Southwest Pacific Ocean), using $^{10}Be/^{9}Be$ dating of entrapped ferromanganese nodules. Mar. Geol. 205 (1–4), 227–247.

Hancock, H.J.L., Dickens, G.R., 2005. Carbonate dissolution episodes in Paleocene and Eocene sediment, Shatsky Rise, west-central Pacific. In: Bralower, T.J., Premoli Silva, I., Malone, M. (Eds.), Ocean Drilling Program, College Station. Proc. ODP, Sci. Results, pp. 1–24. http://dx.doi.org/10.2973/odp.proc.sr.2198.2116.2005.

Haq, B.U., Hardenbol, J.A.N., Vail, P.R., 1987. Chronology of fluctuating sea levels since the Triassic. Science 235, 1156–1167.

Hardenbol, J., Thierry, J., Farley, M.B., de Graciansky, P.-C., Vail, P.R., 1998. Mesozoic and Cenozoic sequence chronostratigraphic framework of European basins. In: de Graciansky, P.-C., Hardenbol, J., Jacquin, T., Vail, P.R. (Eds.), Mesozoic and Cenozoic Sequence Stratigraphy of European Basins. SEPM Special Publication, 60, pp. 3–13.

Harris, A.D., Miller, K.G., Browning, J.V., Sugarman, P.J., Olsson, R.K., Cramer, B.S., Wright, J.D., 2010. Integrated stratigraphic studies of Paleocene–lowermost Eocene sequences, New Jersey Coastal Plain: Evidence for glacioeustatic control. Paleoceanography 25, PA3211.

Hayes, J.M., 1993. Factors controlling ^{13}C contents of sedimentary organic compounds: principles and evidence. Mar. Geol. 113, 111–125.

Hollander, D.J., McKensie, J.A., Hsü, K.J., 1993. Carbon isotope evidence for unusual plankton blooms and fluctuations of surface water CO_2 in "Strangelove Ocean" after terminal Cretaceous event. Palaeogeogr. Palaeoclimatol. Palaeoecol. 104, 229–237.

Hollis, C.J., 2002. Biostratigraphy and paleoceanographic significance of Paleocene radiolarians from offshore eastern New Zealand. Mar. Micropaleontol. 46, 265–316.

Hollis, C.J., 2003. The Cretaceous–Tertiary boundary event in New Zealand: profiling mass extinction. N. Z. J. Geol. Geophys. 46, 307–321.

Hollis, C.J., Manzano-Kareah, K., 2005. Source rock potential of the East Coast Basin (central and northern regions). Ministry of Economic Development Petroleum Report 3179, pp. 1–156.

Hollis, C.J., Beu, A.G., Raine, J.I., Strong, C.P., Turnbull, I.M., Waghorn, D.B., Wilson, G.J., 1997a. Integrated biostratigraphy of Cretaceous–Paleogene strata on Campbell Island, southwest Pacific. Institute of Geological & Nuclear Sciences science report 97/25 (47 pp.).

Hollis, C.J., Waghorn, D.B., Strong, C.P., Crouch, E.M., 1997b. Integrated Paleogene biostratigraphy of DSDP site 277 (Leg 29): foraminifera, calcareous nannofossils, Radiolaria, and palynomorphs. Institute of Geological & Nuclear Sciences science report 97 (7), 1–73.

Hollis, C.J., Dickens, G.R., Field, B.D., Jones, C.J., Strong, C.P., 2005a. The Paleocene–Eocene transition at Mead Stream, New Zealand: a southern Pacific record of early Cenozoic global change. Palaeogeogr. Palaeoclimatol. Palaeoecol. 215, 313–343.

Hollis, C.J., Field, B.D., Jones, C.M., Strong, C.P., Wilson, G.J., Dickens, G.R., 2005b. Biostratigraphy and carbon isotope stratigraphy of uppermost Cretaceous–lower Cenozoic in middle Clarence valley, New Zealand. J. R. Soc. N. Z. 35, 345–383.

Hollis, C.J., Field, B.D., Crouch, E.M., Sykes, R., 2006. How Good a Source Rock is the Waipawa (Black Shale) Formation Beyond the East Coast Basin? New Zealand Petroleum Conference, Auckland, NZ (8 pp.).

Hollis, C.J., Handley, L., Crouch, E.M., Morgans, H.E.G., Baker, J.A., Creech, J., Collins, K.S., Gibbs, S.J., Huber, M., Schouten, S., Zachos, J.C., Pancost, R.D., 2009. Tropical sea temperatures in the high-latitude South Pacific. Geology 37, 99–102.

Hollis, C.J., Taylor, K.W.T., Handley, L., Pancost, R.D., Huber, M., Creech, J., Hines, B., Crouch, E.M., Morgans, H.E.G., Crampton, J.S., Gibbs, S., Pearson, P., Zachos, J.C., 2012. Early Paleogene temperature history of the Southwest Pacific Ocean: reconciling proxies and models. Earth Planet. Sci. Lett. 349–350, 53–66.

Hopmans, E.C., Weijers, J.W.H., Schefuss, E., Herfort, L., Sinninghe Damste, J.S., Schouten, S., 2004. A novel proxy for terrestrial organic matter in sediments based on branched and isoprenoid tetraether lipids. Earth Planet. Sci. Lett. 224, 107–116.

Hornibrook, N.de B., 1992. New Zealand Cenozoic marine paleoclimates: a review based on the distribution of some shallow water and terrestrial biota. In: Tsuchi, R., Ingle, J.C. (Eds.), Pacific Neogene: Environment, Evolution and Events. University of Tokyo Press, Tokyo, pp. 83–106.

Isaac, M.J., Herzer, R.H., Brook, F.J., Hayward, B.W., 1994. Cretaceous and Cenozoic Sedimentary Basins of Northland, New Zealand. Institute of Geological & Nuclear Sciences, Lower Hutt.

Jarvis, I., Lignum, J.S., Gröcke, D.R., Jenkyns, H.C., Pearce, M.A., 2011. Black shale deposition, atmospheric CO_2 drawdown, and cooling during the Cenomanian–Turonian Oceanic Anoxic Event. Paleoceanography 26, PA3201 (doi: 3210.1029/2010PA002081).

Jenkins, D.G., 1968. Planktonic foraminiferida as indicators of New Zealand Tertiary paleotemperatures. Tuatara 16, 32–37.

Kennedy, E.M., 2003. Late Cretaceous and Paleocene terrestrial climates of New Zealand: leaf fossil evidence from South Island assemblages. N. Z. J. Geol. Geophys. 46, 295–306.

Kennett, J.P., et al., 1975. Initial Reports of the Deep Sea Drilling Project, Volume 29. US Govt Printing Office, Washington.

Killops, S.D., Cook, R.A., Sykes, R., Boudou, J.P., 1997. Petroleum potential and oil-source correlation in the Great South and Canterbury basins. N. Z. J. Geol. Geophys. 40 (4), 405–423.

Killops, S.D., Hollis, C.J., Morgans, H.E.G., Sutherland, R., Field, B.D., Leckie, D.A., 2000. Paleoceanographic significance of Late Paleocene dysaerobia at the shelf/slope break around New Zealand. Palaeogeogr. Palaeoclimatol. Palaeoecol. 156, 51–70.

Kim, J.-H., Schouten, S., Hopmans, E.C., Donner, B., Sinninghe Damste, J.S., 2008. Global sediment core-top calibration of the TEX86 paleothermometer in the ocean. Geochim. Cosmochim. Acta 72, 1154–1173.

Kim, J.-H., van der Meer, J., Schouten, S., Helmke, P., Willmott, V., Sangiorgi, F., Koç, N., Hopmans, E.C., Damsté, J.S.S., 2010. New indices and calibrations derived from the distribution of crenarchaeal isoprenoid tetraether lipids: Implications for past sea surface temperature reconstructions. Geochim. Cosmochim. Acta 74, 4639–4654.

King, P.R., Naish, T.R., Browne, G.H., Field, B.D., Edbrooke, S.W., 1999. Cretaceous to Recent sedimentary patterns in New Zealand. Institute of Geological and Nuclear Sciences folio series 1.

Komar, N., Zeebe, R.E., Dickens, G.R., 2013. Understanding long-term carbon cycle trends: the late Paleocene through the early Eocene. Paleoceanography 28, 650–662 (doi: 610.1002/palo.20060).

Kominz, M.A., Browning, J.V., Miller, K.G., Sugarman, P.J., Mizintseva, S., Scotese, C.R., 2008. Late Cretaceous to Miocene sea-level estimates from the New Jersey and Delaware coastal plain coreholes: an error analysis. Basin Res. 20, 211–226.

Leckie, D.A., Morgans, H., Wilson, G.J., Edwards, A.R., 1995. Mid-Paleocene dropstones in the Whangai Formation, New Zealand — evidence of mid-Paleocene cold climate? Sediment. Geol. 97, 119–129.

Lee, J.M., Begg, J.G., 2002. Geology of the Wairarapa area, Institute of Geological & Nuclear Sciences 1:250,000 geological map. Institute of Geological & Nuclear Sciences Limited, Lower Hutt, p. 66 + 61 map.

Liu, Z., Pagani, M., Zinniker, D., DeConto, R., Huber, M., Brinkhuis, H., Shah, S.R., Leckie, R.M., Pearson, A., 2009. Global cooling during the Eocene–Oligocene climate transition. Science 323, 1187–1190.

Lombari, G., Lazarus, D.B., 1988. Neogene cycladophorid radiolarians from the North Atlantic, Antarctic, and North Pacific deep-sea sediments. Micropaleontology 34, 97–135.

Lurcock, P., 2012. Palaeomagnetism of Palaeogene Strata from Southern Zealandia: Implications for Ice in the Greenhouse, PhD Thesis, Geology. University of Otago, Dunedin p. 359.

Miller, K.G., Wright, J.D., Fairbanks, R.G., 1991. Unlocking the ice house: Oligocene–Miocene oxygen isotopes, eustasy, and margin erosion. J. Geophys. Res. 96, 6829–6848.

Miller, K.G., Kominz, M.A., Browning, J.V., Wright, J.D., Mountain, G.S., Katz, M.E., Sugarman, P.J., Cramer, B.S., Christie-Blick, N., Pekar, S.F., 2005. The Phanerozoic record of global sea-level change. Science 310, 1293–1298.

Miller, K.G., Mountain, G.S., Wright, J.D., Browning, J.V., 2011. A 180-million-year record of sea level and ice volume variations from continental margin and deep-sea isotopic records. Oceanography 24, 40–53.

Moore, P.R., 1987. Stratigraphy and structure of the Te Hoe-Waiau River area, western Hawkes Bay. NZ Geol. Surv. Rec. 18, 4–12.

Moore, P.R., 1988. Stratigraphy, composition, and environment of deposition of the Whangai Formation and associated Late Cretaceous–Paleocene rocks, eastern North Island, New Zealand. N. Z. Geol. Surv. Bull. 100.

Moore, P.R., 1989. Stratigraphy of the Waipawa black shale (Paleocene), eastern North Island, New Zealand. NZ Geol. Surv. Rec. 38, 1–19.

Morgans, H.E.G., Jones, C.M., Crouch, E.M., Field, B.D., Hollis, C.J., Raine, J.I., Strong, C.P., Wilson, G.J., 2005. Upper Cretaceous to Eocene stratigraphy and sample collections, mid-Waipara River section, North Canterbury. Institute of Geological and Nuclear Sciences Science Report 2003 (08), 1–107.

Nelson, C.S., Cooke, P.J., 2001. History of oceanic front development in the New Zealand sector of the Southern Ocean during the Cenozoic: a synthesis. N. Z. J. Geol. Geophys. 44 (4), 535–553.

Nicolo, M.J., Dickens, G.R., Hollis, C.J., Zachos, J.C., 2007. Multiple early Eocene hyperthermals: their sedimentary expression on the New Zealand continental margin and in the deep sea. Geology 35 (8), 699–702 (doi:610.1130/G23648A.23641).

Norris, R.D., Kroon, D., Huber, B.T., Erbacher, J., 2001. Cretaceous–Palaeogene ocean and climate change in the subtropical North Atlantic. In: Kroon, D., Norris, R.D., Klaus, A. (Eds.), Western North Atlantic Palaeogene and Cretaceous palaeoceanography. Geological Society Special Publications, pp. 1–22.

Pagani, M., Huber, M., Liu, Z., Bohaty, S.M., Henderiks, J., Sijp, W., Krishnan, S., DeConto, R. M., 2011. The role of carbon dioxide during the onset of antarctic glaciation. Science 334, 1261–1264.

Pancost, R.D., Taylor, K.W.R., Inglis, G.N., Kennedy, E.M., Handley, L., Hollis, C.J., Crouch, E. M., Pross, J., Huber, M., Schouten, S., Pearson, P.N., Morgans, H.E.G., Raine, J.I., 2013. Early Paleogene evolution of terrestrial climate in the SW Pacific, Southern New Zealand. Geochem. Geophys. Geosyst. http://dx.doi.org/10.1002/2013gc004935.

Pekar, S.F., Christie-Blick, N., Kominz, M.A., Miller, K.G., 2002. Calibration between eustatic estimates from backstripping and oxygen isotopic records for the Oligocene. Geology 30, 903–906.

Peterse, F., van der Meer, J., Schouten, S., Weijers, J.W.H., Fierer, N., Jackson, R.B., Kim, J.-H., Sinninghe Damsté, J.S., 2012. Revised calibration of the MBT–CBT paleotemperature proxy based on branched tetraether membrane lipids in surface soils. Geochim. Cosmochim. Acta 96, 215–229.

Petrizzo, M., 2005. An early late Paleocene event on Shatsky Rise, northwest Pacific Ocean (ODP Leg 198): evidence from planktonic foraminiferal assemblages. In: Bralower, T.J., Premoli Silva, I., Malone, M. (Eds.), Ocean Drilling Program, College Station. Proc. ODP, Sci. Results, pp. 1–29. http://dx.doi.org/10.2973/odp.proc.sr.2198.2102.2005.

Rattenbury, M.S., Townsend, D.B., Johnston, M.R., 2006. Geology of the Kaikoura area: scale 1:250,000 geological map. Institute of Geological & Nuclear Sciences, Lower Hutt.

Reay, M.B., 1993. Geology of the middle part of the Clarence Valley, Institute of Geological & Nuclear Sciences geological map 10. Institute of Geological & Nuclear Sciences, Lower Hutt.

Rhodes, G.M., Ali, J.R., Hailwood, E.A., King, C., Gibson, T.G., 1999. Magnetostratigraphic correlation of Paleogene sequences from northwest Europe and North America. Geology 27, 451–454.

Rogers, K.M., Morgans, H.E.G., Wilson, G.S., 2001. Identification of a Waipawa Formation equivalent in the upper Te Uri Member of the Whangai Formation: implications for depositional history and age. N. Z. J. Geol. Geophys. 44 (2), 347–354.

Röhl, U., Brinkhuis, H., Sluijs, A., Fuller, M., 2004. On the search for the Paleocene/Eocene boundary in the Southern Ocean: exploring ODP Leg 189 Holes 1171D and 1172D, Tasman Sea. In: Exon, N.F., Kennett, J.P., Malone, M.J. (Eds.), The Cenozoic Southern Ocean: Tectonics, Sedimentation, and Climate Change Between Australia and Antarctica. AGU Geophysical Monograph, 151, pp. 113–126.

Rullkötter, J., 2000. Organic matter: the driving force for early diagnesis. In: Zabel, M., Schulz, H.D. (Eds.), Marine Geochemistry. Springer-Verlag, pp. 129–172.

Schiøler, P., Rogers, K., Sykes, R., Hollis, C.J., Ilg, B., Meadows, D., Roncaglia, L., Uruski, C., 2010. Palynofacies, organic geochemistry and depositional environment of the Tartan Formation (Late Paleocene), a potential source rock in the Great South Basin, New Zealand. Mar. Pet. Geol. 27, 351–369.

Schlanger, S.O., Jenkyns, H.C., 1976. Cretaceous oceanic anoxic events: causes and consequences. Geol. Mijnb. 55, 179–184.

Schmitz, B., Pujalte, V., Molina, E., Monechi, S., Orue-Etxebarria, X., Speijer, R.P., Alegret, L., et al., 2011. The global stratotype sections and points for the bases of the Selandian (Middle Paleocene) and Thanetian (Upper Paleocene) stages at Zumaia, Spain. Episodes 34, 220–243.

Schouten, S., Hopmans, E.C., Schefuß, E., Sinninghe Damsté, J.S., 2002. Distributional variations in marine crenarchaeotal membrane lipids: a new tool for reconstructing ancient sea water temperatures? Earth Planet. Sci. Lett. 204, 265–274.

Schouten, S., Hopmans, E.C., Sinninghe Damsté, J.S., 2013. The organic geochemistry of glycerol dialkyl glycerol tetraether lipids: A review. Organic Geochemistry 54, 19–61.

Shackleton, N.J., 1986. Paleogene stable isotopes events. Palaeogeogr. Palaeoclimatol. Palaeoecol. 57, 91–102.

Sinninghe Damsté, J.S., Kok, M.D., Köster, J., Schouten, S., 1998. Sulfurized carbohydrates: an important sedimentary sink for organic carbon? Earth Planet. Sci. Lett. 164, 7–13.

Slotnick, B.S., Dickens, G.R., Nicolo, M., Hollis, C.J., Crampton, J.S., Zachos, J.C., Sluijs, A., 2012. Numerous large amplitude variations in carbon cycling and terrestrial weathering throughout the latest Paleocene and earliest Eocene. J. Geol. 120, 487–505.

Sluijs, A., Dickens, G.R., 2012. Assessing offsets between the δ^{13}C of sedimentary components and the global exogenic carbon pool across early Paleogene carbon cycle perturbations. Glob. Biogeochem. Cycles 26, GB4005 (doi: 4010.1029/2011gb004224).

Sluijs, A., Brinkhuis, H., Crouch, E.M., John, C.M., Handley, L., Munsterman, D., Bohaty, S.M., Zachos, J.C., Reichart, G.-J., Schouten, S., Pancost, R.D., Damsté, J.S.S., Welters, N.L.D., Lotter, A.F., Dickens, G.R., 2008. Eustatic variations during the Paleocene–Eocene greenhouse world. Paleoceanography 23, PA4216. http://dx.doi.org/10.1029/2008pa001615.

Sluijs, A., Bijl, P.K., Schouten, S., Roehl, U., Reichart, G.J., Brinkhuis, H., 2011. Southern ocean warming, sea level and hydrological change during the Paleocene–Eocene thermal maximum. Clim. Past 7, 47–61.

Spofforth, D.J.A., Agnini, C., Pälike, H., Rio, D., Fornaciari, E., Giusberti, L., Luciani, V., Lanci, L., Muttoni, G., 2010. Organic carbon burial following the middle Eocene climatic optimum in the central western Tethys. Paleoceanography 25, PA3210.

Stickley, C.E., Brinkhuis, H., Schellenberg, S.A., Sluijs, A., Röhl, U., Fuller, M., Grauert, M., Huber, M., Warnaar, J., Williams, G.L., 2004. Timing and nature of the deepening of the Tasmanian Gateway. Paleoceanography 19, PA4027 (doi:4010.1029/2004PA001022).

Stocchi, P., Escutia, C., Houben, A.J.P., Vermeersen, B.L.A., Bijl, P.K., Brinkhuis, H., DeConto, R.M., Galeotti, S., Passchier, S., Pollard, D., Klaus, A., Fehr, A., Williams, T., Bendle, J.A.P., Bohaty, S.M., Carr, S.A., Dunbar, R.B., Flores, J.A., Gonzàlez, J.J., Hayden, T.G., Iwai, M., Jimenez-Espejo, F.J., Katsuki, K., Kong, G.S., McKay, R.M., Nakai, M., Olney, M.P., Pekar, S.F., Pross, J., Riesselman, C., Röhl, U., Sakai, T., Shrivastava, P.K., Stickley, C.E., Sugisaki, S., Tauxe, L., Tuo, S., van de Flierdt, T., Welsh, K., Yamane, M., 2013. Relative sea-level rise around East Antarctica during Oligocene glaciation. Nat. Geosci. 6, 380–384.

Tayler, M.J.S., 2011. Investigating Stratigraphic Evidence for Antarctic glaciation in the Greenhouse World of the Paleocene, Eastern North Island, New Zealand, MSc Thesis, Earth and Ocean Sciences. University of Waikato, Hamilton p. 292.

Taylor, K., 2011. Paleocene Climate and Carbon Cycle: Insights into an Unstable Greenhouse from a Biomarker and Compound Specific Carbon Isotope Approach, PhD Thesis. University of Bristol, Bristol p. 310.

Taylor, K.W.R., Huber, M., Hollis, C.J., Hernandez-Sanchez, M.T., Pancost, R.D., 2013. Re-evaluating modern and Palaeogene GDGT distributions: implications for SST reconstructions. Glob. Planet. Chang. 108, 158–174 (doi: 110.1016/j.gloplacha.2013.1006.1011).

Thompson, E.I., Schmitz, B., 1997. Barium and the late Paleocene δ^{13}C maximum: evidence of increased marine surface productivity. Paleoceanography 12, 239–254.

Turich, C., Freeman, K.H., Bruns, M.A., Conte, M., Jones, A.D., Wakeham, S.G., 2007. Lipids of marine Archaea: patterns and provenance in the water-column and sediments. Geochim. Cosmochim. Acta 71, 3272–3291.

Wei, K.Y., Mii, H.S., Shu, I.T., Lin, Y.J., 2005. Uppermost Cretaceous to Middle Oligocene carbon and oxygen isotope stratigraphy of Southwest Pacific: holes 1121B and 1124C, ODP Leg 181. N. Z. J. Geol. Geophys. 48 (1), 15–26.

Weijers, J.W.H., Schouten, S., van den Donker, J.C., Hopmans, E.C., Sinninghe Damste, J.S., 2007. Environmental controls on bacterial tetraether membrane lipid distribution in soils. Geochim. Cosmochim. Acta 71, 703–713.

Westerhold, T., Röhl, U., Raffi, I., Fornaciari, E., Monechi, S., Reale, V., Bowles, J., Evans, H.F., 2008. Astronomical calibration of the Paleocene time. Palaeogeogr. Palaeoclimatol. Palaeoecol. 257, 377–403.

Westerhold, T., Röhl, U., Donner, B., McCarren, H.K., Zachos, J.C., 2011. A complete high-resolution Paleocene benthic stable isotope record for the central Pacific (ODP Site 1209). Paleoceanography 26, PA2216.

Wilson, D.S., Luyendyk, B.P., 2009. West Antarctic paleotopography estimated at the Eocene–Oligocene climate transition. Geophys. Res. Lett. 36 (L16302), 16301–16304 (doi:16310.11029/12009GL039297).

Wilson, G.J., Moore, P.R., 1988. Cretaceous–Tertiary boundary in the Te Hoe River area, western Hawkes Bay. NZ Geol. Surv. Rec. 35, 34–37.

Wilson, D.S., Pollard, D., DeConto, R.M., Jamieson, S.S.R., Luyendyk, B.P., 2013. Initiation of the West Antarctic Ice Sheet and estimates of total Antarctic ice volume in the earliest Oligocene. Geophys. Res. Lett. 40, 4305–4309 (doi: 4310.1002/grl.50797).

Zachos, J., Pagani, M., Sloan, L., Thomas, E., Billups, K., 2001. Trends, rhythms, and aberrations in global climate 65 Ma to present. Science 292, 686–693.

Zachos, J.C., Dickens, G.R., Zeebe, R.E., 2008. An early Cenozoic perspective on greenhouse warming and carbon-cycle dynamics. Nature 451, 279–283.